Proficient multivariate approach for iron(II) spin crossover behaviour modelling in the solid state

Lorenzo Marchi, Simone Fantuzzi, Andrea Cingolani, Alessandro Messori, Rita Mazzoni, Stefano Zacchini, Marina Cocchi and Luca Rigamonti

ELECTRONIC SUPPLEMENTARY INFORMATION (ESI)

Index

Table S1 Rules for the three-letter labels of the iron(II) complexes, where the first letter+number combination identifies the substituent R (H = hydrogen, X = halogens, N = substituents bound through nitrogen to the pyridyl ring, O = substituents bound through oxygen to the pyridyl ring, S = substituents bound through sulphur to the pyridyl ring, C = substituents bound through carbon to the pyridyl ring, A = bound substituted aromatic rings, M = substituents containing fragments with coordinated metal ions), the second letter represents the anion X^-, and the third letter the co-crystallized solvent. For example, **H01AA** corresponds to $[Fe(bpp\text{-}H)_2](BF_4)_2$ without co-crystallized solvent molecules (solvent free, SF), while **C01BC** corresponds to $[Fe(bpp\text{-}Me)_2](BF_4)_2{\cdot}4MeNO_2$; when more than one type of co-crystallized solvent is present, the letter identifies the one in the highest amount. Graphical representation of the substituents R and anions $[Ni(mnt)_2]^-$ and $[Co(carborane)_2]^-$ is reported in Fig. S1. The substituents in italics and red do not have any crystal structure determination available.

Letter+number	Substituent R
H01	H
X01	F
X02	Cl
X03	Br
X04	I
N01	NH_2
N02	NMe_2
N03	*NO_2*
N04	NHCOMe
N05	Thiomorpholine
N06	*E*-N=N–Ph
O01	OH
O02	OMe
S01	*SH*
S02	SMe
S03	S–*i*Pr
S04	S–*t*Bu
S05	*SOMe*
S06	*SO_2Me*
S07	*$S(CH_2)_2NHC(O)(CH_2)_4(C_3H_5S_2)$*
S08	*bridging S–S (proposed tetranuclear iron(II) compound)*
C01	Me
C02	CH_2OH
C03	CH_2Br
C04	CH_2SCN
C05	C≡N
C06	COOH

C07	COOH (on position 3)
C08	COOMe
C09	COOMe (on position 3)
C10	COOEt
C11	$CONH(CH_2OH)_3$
C12	$CONHCH_2COOH$
C13	$CONH(CH_2)_2COOH$
C14	$CSNH_2$
C15	CSNHMe
C16	$COOC_6H_4OH$
C17	$COOC_6H_4OMe$
C18	$COOC_6H_3(OH)_2$
C19	$COOC_6H_3(OMe)_2$
C20	$COOC_6H_4OC_6H_{13}$
C21	$COOC_6H_4OC_{12}H_{25}$
C22	$COOC_6H_4OC_{14}H_{29}$
C23	$COOC_6H_4OC_{16}H_{33}$
C24	$COOC_6H_4OC_{18}H_{37}$
C25	$COOCH_2Ph$
C26	$COOCH_2C_6H_4OMe$
C27	$COOCH_2C_6H_3(OMe)_2$
C28	$COOC_{12}H_{25}$
C29	$COOC_{14}H_{29}$
C30	$COOC_{16}H_{33}$
C31	$COOC_{18}H_{37}$
C32	C≡CH
C33	$C{\equiv}C–SiMe_3$
C34	C≡C–SC(O)Me
C35	C≡C–Ph
C36	$C{\equiv}C–C_6H_4SC(O)Me$
C37	bridging C≡C–anthracene-C≡C (tetranuclear iron(II) compound)
C38	bridging C≡C–anthracene–C≡C–anthraquinone–C≡C–anthracene–C≡C (hexanuclear iron(II) compound)
C39	*E*-CH=CH–Ph
C40	*Z*-CH=CH–Ph
C41	*E*-$CH{=}CH–C_6H_4CN$
C42	*Z*-$CH{=}CH–C_6H_4CN$
C43	*E*-$CH{=}CH–C_6H_4NO_2$
C44	*Z*-$CH{=}CH–C_6H_4NO_2$
C45	*E*-CH=CH–Fc
C46	*E*-CH=CH–Tetrathiofulvalene (TTF)
C47	Nitrosyl nitroxide
C48	$CH_2OC(O)(CH_2)_3$*pyrene*
C49	$COO(CH_2)_4$*pyrene*
C50	$COOCH_2$*pyrene*
C51	$CH_2OC(O)CH_2$*pyrene*

C52	*$CH_2OC(O)(CH_2)_4(C_3H_5S_2)$*
C53	*$CONH(CH_2)_2OC(O)(CH_2)_4(C_3H_5S_2)$*
C54	*$COO(CH_2)_2OC(O)(CH_2)_4(C_3H_5S_2)$*
A01	4-C_6H_4OH
A02	4-C_6H_4CHO
A03	4-$C_6H_4C{\equiv}N$
A04	Pyrazol-1-yl
A05	Imidazol-1-yl
A06	Pyrid-4-yl
A07	Pyrid-3-yl
A08	Pyrene
A09	*Cyclotriphosphazene (CTPZ)*
A10	*4-$C_6H_4CH_2OC(O)C$(fullerene)$COOEt$*
M01	C≡C–Pt(4-*t*Bu-Terpy)
M02	*$CONHC(CH_2O)_3POM$, POM = $MnMo_6O_{24}$ (1D polymeric chain)*

Letter label	Anion X^-
A	BF_4^-
B	ClO_4^-
C	TfO^-
D	PF_6^-
E	AsF_6^-
F	SbF_6^-
G	BPh_4^-
H	I^-/I_3^-
I	$[Ni(mnt)_2]^-$ (mnt = maleonitriledithiolate)
J	$[Co(carborane)_2]^-$

Letter label	Solvent
A	SF (solvent free)
B	H_2O
C	$MeNO_2$
D	MeCN
E	Me_2CO
F	MeOH
G	Et_2O
H	CH_2Cl_2
I	EtCN
J	PhCN
K	Propylene carbonate (PC)

a)

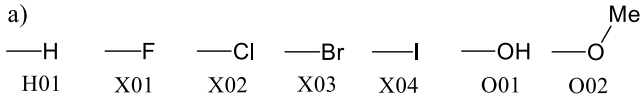
H01
X01
X02
X03
X04
O01
O02

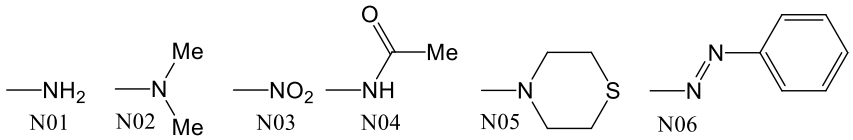
N01
N02
N03
N04
N05
N06

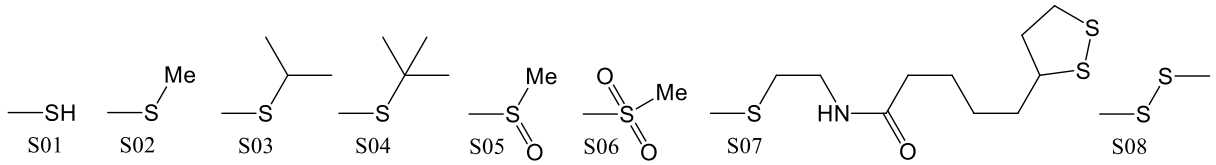
S01
S02
S03
S04
S05
S06
S07
S08

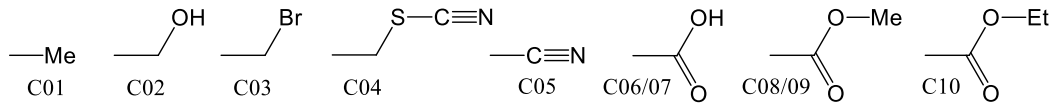
C01
C02
C03
C04
C05
C06/07
C08/09
C10

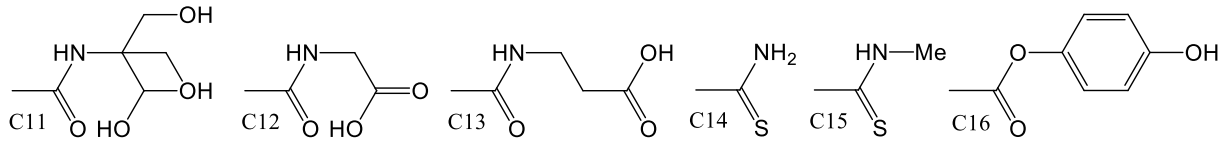
C11
C12
C13
C14
C15
C16

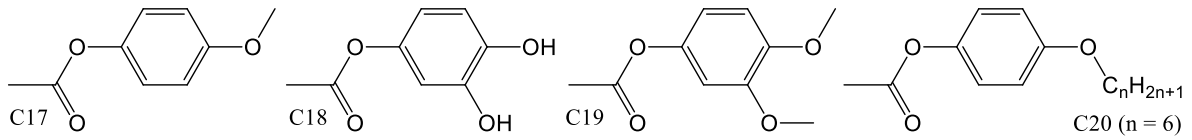
C17
C18
C19
C20 (n = 6)
C21 (n = 12)
C22 (n = 14)
C23 (n = 16)
C24 (n = 18)

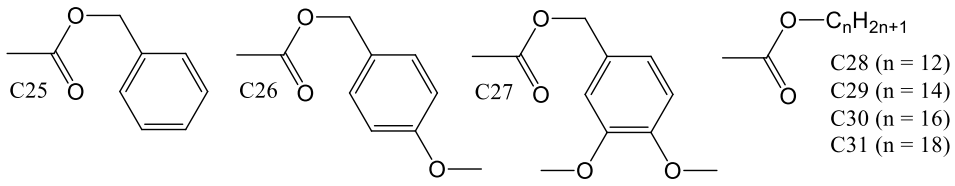
C25
C26
C27
C28 (n = 12)
C29 (n = 14)
C30 (n = 16)
C31 (n = 18)

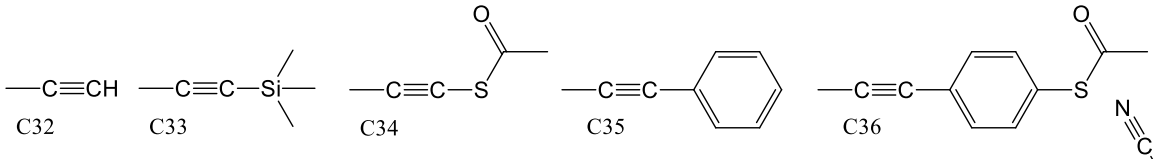
C32
C33
C34
C35
C36

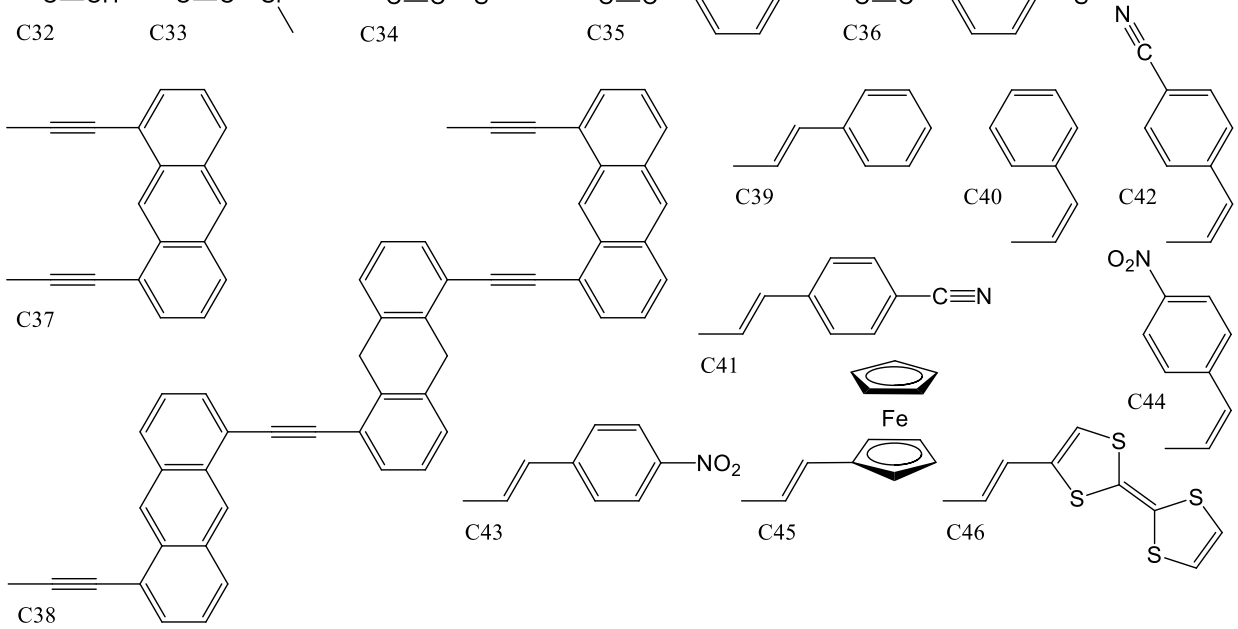
C37
C38
C39
C40
C41
C42
C43
C44
C45
C46
Fe

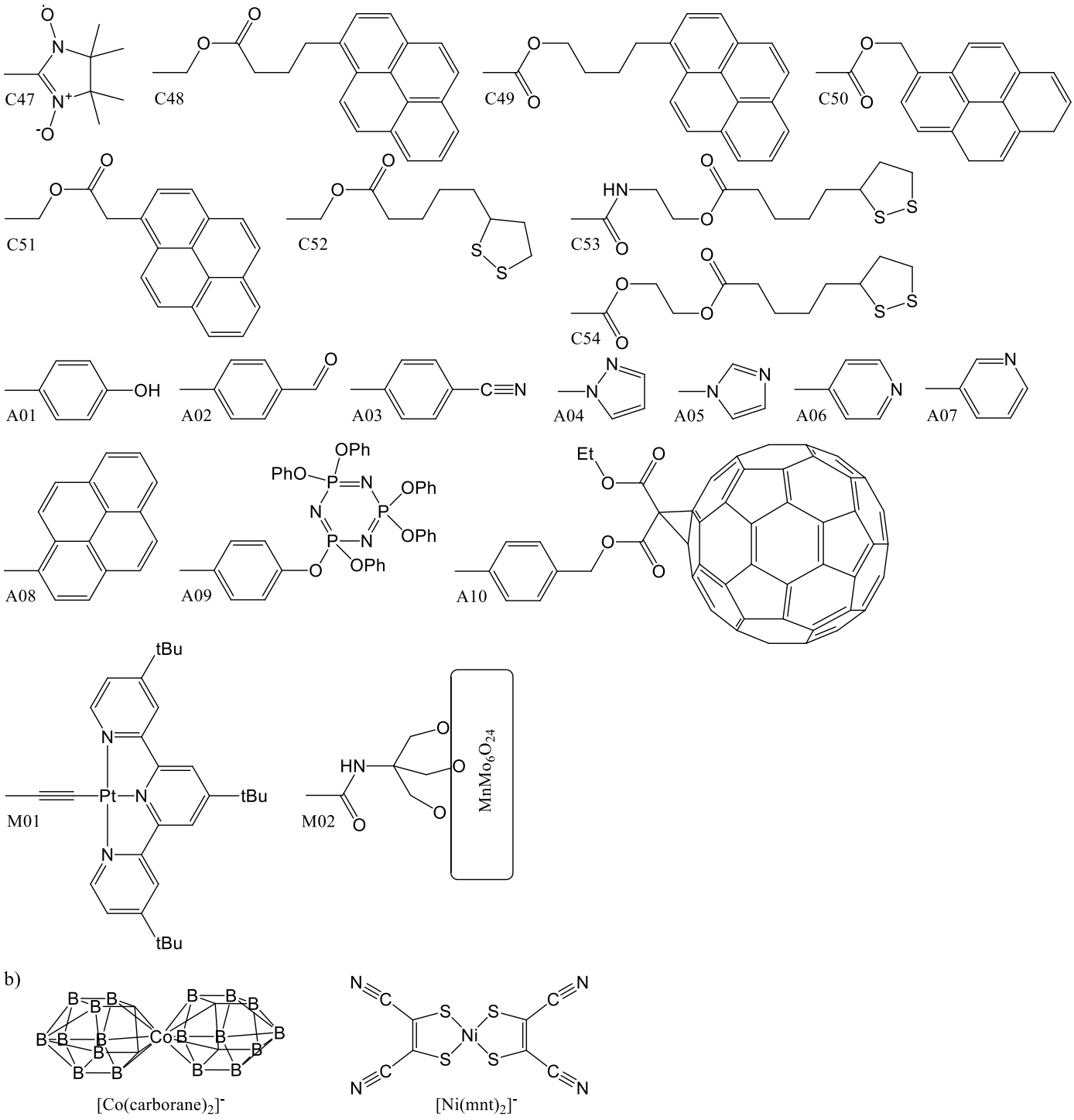

Fig. S1 Drawing of the a) substituents R of complexes $[Fe(bpp\text{-}R)_2](X)_2 \cdot$solvent with relative letter+number coding, and b) $[Co(carborane)_2]^-$ and $[Ni(mnt)_2]^-$ anions.

Table S2 Iron(II) complexes $[Fe(bpp\text{-}R)_2](X)_2 \cdot$solvent known in the literature. The compounds in bold are the ones employed in this study.

label	year	R	X^-	solvent	CCDC/CSD	T_{RX} (K)	Spin state	SCO	ref
H01AA	2001	H	BF_4^-	SF	158392 XENBEX01	375	HS	Yes (261)	[1]
H01AA	2001	H	BF_4^-	SF	158393 XENBEX	290	HS	Yes (261)	[1]
H01AA	2001	H	BF_4^-	SF	158394 XENBEX02	240	LS	Yes (261)	[1]
H01AA	2001	H	BF_4^-	SF	158395 XENBEX03	150	LS	Yes (261)	[1]
H01AC	2002	H	BF_4^-	$2.9CH_3NO_2$ $0.25H_2O$	171144 ADIYOB	150	LS	Yes (≈260) [a1]	[2]
H01DA	2002	H	PF_6^-	SF	171145 ADIYUH	120	HS	No (HS)	[2]
H01AA	2003	H	BF_4^-	SF	195715 XENBEX04	30	LS	Yes (261)	[3]
H01AA	2003	H	BF_4^-	SF	195714 XENBEX05	30	HS [a2]	Yes (261) LIESST	[3]
C02AA	2004	CH_2OH	BF_4^-	SF	229751 IYUFOX01	300	HS	Yes (271)	[4]
C02AA	2004	CH_2OH	BF_4^-	SF	229749 IYUFOX	30	LS	Yes (271)	[4]
C02AA	2004	CH_2OH	BF_4^-	SF	229750 IYUFOX02	30	HS [a2]	Yes (271) LIESST	[4]
H01BA	2005	H	ClO_4^-	SF	263420 GAPSIA	150	HS	No (HS)	[5]
H01FA	2005	H	SbF_6^-	SF	263421 GAPSOG	150	HS	No (HS)	[5]
H01HA	2006	H	$0.5I^- 1.5I_3^-$	SF	278897 ECELAA	150	HS	No (HS)	[6]
H01JC	2006	H	$[Co(carborane)_2]^{2-}$	CH_3NO_2	278898 ECELEE	300	mixed [a3]	Partial (50%, 300)	[6]
H01JC	2006	H	$[Co(carborane)_2]^{2-}$	CH_3NO_2	278899 ECELEE01	150	mixed [a3]	Partial (300, 50%)	[6]
C02BA	2006	CH_2OH	ClO_4^-	SF	296687 NESVOX	340	HS	Yes (284)	[7]
C02BA	2006	CH_2OH	ClO_4^-	SF	296688 NESVOX01	30	LS	Yes (284)	[7]
C02BA	2006	CH_2OH	ClO_4^-	SF	296689 NESVOX02	30	HS [a2]	Yes (284) (LIESST)	[7]
A06BF	2006	py (4)	ClO_4^-	MeOH	234927 CETYIK	180	LS	Yes (287) [a4]	[8]

H01AA	2007	H	BF_4^-	SF	631320 XENBEX06	300	HS	Yes (259) [a5]	9
H01AA	2007	H	BF_4^-	SF	631321 XENBEX07	150	LS	Yes (259) [a5]	9
A03AD	2007	C_6H_4CN (4)	BF_4^-	2MeCN	634174 YIKNUC	180	LS [a6]	Yes (166) [a7]	10
A03AD	2007	C_6H_4CN (4)	BF_4^-	2MeCN	634175 YIKNUC01	180	LS [a6]	Yes (166) [a7]	10
A03AD	2007	C_6H_4CN (4)	ClO_4^-	2MeCN	634176 YIKPAK	150	LS	Yes (179) [a7]	10
C45AG	2007	*E*-CH=CH-Fc	BF_4^-	$2Et_2O$	829371 ARIXEF	110	HS	Partial <20% (≈100)	11
C45AG	2007	*E*-CH=CH-Fc	BF_4^-	Et_2O	829372 ARIXIJ	110	LS	Yes (230)	11
C45AG	2007	*E*-CH=CH-Fc	BF_4^-	Et_2O	829373 ARIXIJ01	293	HS / mixed	Yes (230)	11
C47AE	2007	Nitrosyl nitroxide	BF_4^-	Me_2CO	278362 TICXUZ	200	LS	No (LS up to RT)	12
X04BA	2008	I	ClO_4^-	SF	682057 COMRAY	180	LS	Yes (333)	13
A01BA	2008	4-C_6H_4OH	ClO_4^-	SF	682058 COMREC	180	LS	Yes (281)	13
C33BD	2008	C≡C-$SiMe_3$	ClO_4^-	2MeCN	682059 COMRIG	180	mixed	Partial 50% (≈220)	13
C33BD	2008	C≡C-$SiMe_3$	ClO_4^-	2MeCN	not deposited	298	HS	Partial 50% (≈220)	13
C32BA	2008	C≡CH	ClO_4^-	SF	682060 COMROM	180	LS	No (LS up to 380 K)	13
C36BH	2008	C≡C-C_6H_4 SC(O)Me	ClO_4^-	$3CH_2Cl_2$	668334 XOCFIF	180	LS	Yes (277)	14
C45HA	2008	*E*-CH=CH-Fc	I_3^-	SF	676598 POLLAE	200	HS	No (HS)	15
C45GC	2008	*E*-CH=CH-Fc	BPh_4^-	$3MeNO_2$ Et_2O	676599 POLLEI	200	HS	No (HS)	15
C45IA	2008	*E*-CH=CH-Fc	$[Ni(mnt)_2]^-$	SF	676600 POLLIM	200	HS	No (HS)	15
H01HA	2009	H	I_3^-	SF	734793 OZOGIV	293	HS	No (HS)	16
H01AA	2009	H	BF_4^-	SF	722725 XENBEX08	300	HS	Yes (259) [a8]	17
C04AA	2009	CH_2SCN	BF_4^-	SF	699523 FOYYAU	100	HS	No (HS) [a9]	18
C04AA	2009	CH_2SCN	BF_4^-	SF	699524 FOYYAU01	313	HS	No (HS)	18
C04AA	2009	CH_2SCN	BF_4^-	SF	699525 FOYYAU02	100	LS	Yes (272) [a9]	18

C04AA	2009	CH_2SCN	BF_4^-	SF	699526 FOYYAU03	150	LS	Yes (272)	[18]
C04AA	2009	CH_2SCN	BF_4^-	SF	699527 FOYYAU04	200	LS	Yes (272)	[18]
C04AA	2009	CH_2SCN	BF_4^-	SF	699528 FOYYAU05	278	HS / mixed	Yes (272)	[18]
C04AA	2009	CH_2SCN	BF_4^-	SF	699529 FOYYAU06	313	HS	Yes (272)	[18]
A07BA	2010	py (3)	ClO_4^-	SF	764304 YUZTIX	180	LS	Yes (406)	[19]
A07AA	2010	py (3)	BF_4^-	SF	764305 YUZTOD	180	LS	Yes (400)	[19]
A07AB	2010	py (3)	BF_4^-	H_2O MeCN	764306 YUZTUJ	180	LS	Yes (≈300) [a10]	[19]
H01IC	2010	H	$[Ni(mnt)_2]^-$	$MeNO_2$	691358 LUXMOH	200	HS	Yes (175)	[20]
H01IC	2010	H	$[Ni(mnt)_2]^-$	$MeNO_2$	691359 LUXMOH01	140	LS	Yes (175)	[20]
H01IC	2010	H	$[Ni(mnt)_2]^-$	$MeNO_2$	691360 LUXMOH02	205	HS	Yes (175)	[20]
H01IC	2010	H	$[Ni(mnt)_2]^-$	$MeNO_2$	691361 LUXMOH03	293	HS	Yes (175)	[20]
H01IC	2010	H	$[Ni(mnt)_2]^-$	$MeNO_2$	780979 LUXMOH04	180	mixed	Yes (175)	[20]
C40AA	2011	*Z*-CH=CH-Ph	BF_4^-	SF	811070 ITECOA	90	HS	No (HS)	[21]
C39AK	2011	*E*-CH=CH-Ph	BF_4^-	2PC [a11]	811071 ITECUG	113	LS	Not tested [a11]	[21]
C46GC	2011	TTF [a12]	BPh_4^-	$MeNO_2$ ½Et_2O	796347 AMIHUA	120	LS	Yes (≈200)	[22]
C46IJ	2011	TTF [a12,a13]	$2[Ni(mnt)_2]^-$ BF_4^-	PhCN	796348 AMIJAI	200	LS	Yes (≈240)	[22]
C46IJ	2011	TTF [a12,a13]	$2[Ni(mnt)_2]^-$ BF_4^-	PhCN	796349 AMIJAI01	300	HS (mixed)	Yes (≈240)	[22]
A08BA	2011	pyrene	ClO_4^-	SF	790319 OVEPAH	180	HS	No (HS)	[23]
C48AA	2011	chain pyrene [a14]	BF_4^-	SF	-	-	-	Yes (216)	[23]
C48AB	2011	chain pyrene [a14]	BF_4^-	H_2O MeCN	-	-	-	Yes (218)	[23]
C32AA	2012	C≡CH	BF_4^-	SF	846470 CAQFEH	180	LS	Yes (340) [a15]	[24]
C32AA	2012	C≡CH	BF_4^-	SF	846471 CAQFEH01	350	LS (mixed)	Yes (340) [a15]	[24]
C32AA	2012	C≡CH	BF_4^-	SF	846472 CAQFEH02	180	LS	Yes (≈450) [a15]	[24]

C32AA	2012	C≡CH	BF_4^-	SF	846473 CAQFEH03	370	HS	Yes (340) [a15]	24
C40AA	2012	*Z*-CH=CH-Ph	BF_4^-	SF	811070 ITECOA	90	HS	No (HS)	25
C42AA	2012	*Z*-CH=CH-C_6H_4CN	BF_4^-	SF	892107 GAYBUF	113	HS	No (HS)	25
C44AE	2012	*Z*-CH=CH-$C_6H_4NO_2$	BF_4^-	Me_2CO	892108 GAYGAM	113	LS	Yes (>300)	25
C41AC	2012	*E*-CH=CH-C_6H_4CN	BF_4^-	$MeNO_2$	892109 GAYCEQ	113	LS	Partial [a16]	25
C43AB	2012	*E*-CH=CH-$C_6H_4NO_2$	BF_4^-	H_2O	892110 GAYCIU	113	HS	Partial [a16]	25
A02BA	2013	4-C_6H_4CHO	ClO_4^-	SF	899972 ZERWEA	180	LS	Yes (285)	26
C39AK	2013	*E*-CH=CH-Ph	BF_4^-	2PC [a11]	811071 ITECUG	113	LS	No (LS up to RT)	27
C39AK	2013	*E*-CH=CH-Ph	BF_4^-	2PC [a11]	911443 ITECUG01	283	LS	No (LS up to RT)	27
C39AG	2013	*E*-CH=CH-Ph	BF_4^-	½Et_2O	911442 REVCIG	113	LS	No (LS up to RT)	27
C39AD	2013	*E*-CH=CH-Ph	BF_4^-	3MeCN H_2O	911441 REVCOM	113	HS	No (HS)	27
C39AC	2013	*E*-CH=CH-Ph	BF_4^-	4$MeNO_2$	911440 REVCUS	243	HS	Yes (≈220) [a17]	27
C39AC	2013	*E*-CH=CH-Ph	BF_4^-	4$MeNO_2$	911439 REVCUS01	217	Mixed	Yes (≈220) [a17]	27
C39AC	2013	*E*-CH=CH-Ph	BF_4^-	4$MeNO_2$	911438 REVCUS02	192	LS	Yes (≈220) [a17]	27
C39AC	2013	*E*-CH=CH-Ph	BF_4^-	4$MeNO_2$	911437 REVCUS03	165	LS	Yes (≈220) [a17]	27
C39AC	2013	*E*-CH=CH-Ph	BF_4^-	4$MeNO_2$	911436 REVCUS04	140	LS	Yes (≈220) [a17]	27
C39AC	2013	*E*-CH=CH-Ph	BF_4^-	4$MeNO_2$	911435 REVCUS05	115	LS	Yes (≈220) [a17]	27
C39AC	2013	*E*-CH=CH-Ph	BF_4^-	4$MeNO_2$	911434 REVCUS06	113 [a18]	LS	Yes (≈220) [a17]	27
C39AE	2013	*E*-CH=CH-Ph	BF_4^-	Me_2CO	911433 REVFEF	240	HS	Yes (≈180)	27
C39AE	2013	*E*-CH=CH-Ph	BF_4^-	Me_2CO	911432 REVFEF01	190	HS	Yes (≈180)	27
C39AE	2013	*E*-CH=CH-Ph	BF_4^-	Me_2CO	911431 REVFEF02	175	LS	Yes (≈180)	27
C39AE	2013	*E*-CH=CH-Ph	BF_4^-	Me_2CO	911430 REVFEF03	150	LS	Yes (≈180)	27
C39AE	2013	*E*-CH=CH-Ph	BF_4^-	Me_2CO	911429 REVFEF04	113 [a18]	HS	Yes (≈180)	27
A09BA	2013	CTPZ [a19]	ClO_4^-	SF	-	-	-	No (HS)	28

C06BA	2014	COOH	ClO_4^-	SF	977453 BIYSOT	120	LS	Yes (380)	[29]
S02AA	2015	SMe	BF_4^-	SF	1006370 MUCREJ	100	LS	Yes (268)	[30]
S02AA	2015	SMe	BF_4^-	SF	1006371 MUCREJ01	240	LS mixed	Yes (268)	[30]
S02AA	2015	SMe	BF_4^-	SF	1006372 MUCREJ02	290	HS	Yes (268)	[30]
X03AA	2015	Br	BF_4^-	SF	1006373 MUCRUZ	100	LS	Yes (307)	[30]
X03AA	2015	Br	BF_4^-	SF	1006374 MUCRUZ01	250	LS	Yes (307)	[30]
X03AA	2015	Br	BF_4^-	SF	1006375 MUCRUZ02	350	HS	Yes (307)	[30]
X04AA	2015	I	BF_4^-	SF	1006376 MUCSIO	100	LS	Yes (332)	[30]
X04AA	2015	I	BF_4^-	SF	1006377 MUCSIO01	350	HS	Yes (332)	[30]
C35AC	2015	C≡C-Ph	BF_4^-	$MeNO_2$	1004453 XUKDEO	150	HS	No (HS)	[31]
N06AC	2015	N=N-Ph	BF_4^-	$MeNO_2$	1004454 XUKDIS	150	LS	No (LS up to RT	[31]
A04AC	2015	Pyrazol-1-yl	BF_4^-	½$MeNO_2$	1004455 XUKDOI	100	mixed [a20]	Partial (65%) (250)	[31]
A04AC	2015	Pyrazol-1-yl	BF_4^-	2$MeNO_2$	1004456 XUKDUE	100	LS	No (LS up to RT)	[31]
A04AC	2015	Pyrazol-1-yl	BF_4^-	3$MeNO_2$	1004457 XUKFAM	100	LS	Yes (*T* not reported)	[31]
A04DC	2015	Pyrazol-1-yl	PF_6^-	2$MeNO_2$	1004459 XUKGEQ	105	LS	No (LS up to RT) [a21]	[31]
H01AF	2015	H	BF_4^-	MeOH	1004460 XUKFIU	120	LS	No (LS up to RT)	[31]
S01AA	2015	SH	BF_4^-	SF	-	-	-	Partial (≈275)	[32]
S01BA	2015	SH	ClO_4^-	SF	-	-	-	Yes (≈250)	[32]
S08AA	2015	S-S [a22]	BF_4^-	SF	-	-	-	Partial (broad 50%)	[32]
S08BA	2015	S-S [a22]	ClO_4^-	SF	-	-	-	Partial (broad 50%)	[32]
S02BA	2015	SMe	ClO_4^-	SF	1060841 VULNIB	280	HS	Yes (≈250)	[33]
S02BA	2015	SMe	ClO_4^-	SF	1060842 VULNIB02	253	HS mixed	Yes (≈250)	[33]
S02BA	2015	SMe	ClO_4^-	SF	1060843 VULNIB01	240	LS	Yes (≈250)	[33]
S02BA	2015	SMe	ClO_4^-	SF	1060844 VULNIB03	150	LS	Yes (≈250)	[33]

S05AB	2015	SOMe	BF_4^-	$2H_2O$	-	-	-	Yes (350)	[33]
S06AA	2015	SO_2Me	BF_4^-	SF	-	-	-	Yes (> 350)	[33]
C01AC	2015	Me	BF_4^-	$4MeNO_2$	1006380 CUKVUB	100	LS	No (LS up to RT)	[34]
C01AA	2015	Me	BF_4^-	SF	-	-	-	Yes (204,209)	[34]
C01BC	2015	Me	ClO_4^-	$4MeNO_2$	1006381 CUKWAI	150	LS	No (LS up to RT)	[34]
C01BA	2015	Me	ClO_4^-	SF	1006382 CUKWEM	100	HS [a23]	Yes (175,193)	[34]
C01BA	2015	Me	ClO_4^-	SF	1006383 CUKWEM01	240	HS	Yes (175,193)	[34]
C01DA	2015	Me	PF_6^-	SF	1006384 CUKWOW	100	HS	No (HS)	[34]
C01CB	2015	Me	TfO^-	$½H_2O$	-	-	-	No (LS up to RT)	[34]
N05AB	2015	thiomorpholine	BF_4^-	H_2O	1058749 MUJWOF	100	HS	No (HS)	[35]
N05BB	2015	thiomorpholine	ClO_4^-	$⅓H_2O$	1058750 MUJWUL	100	HS	No (HS)	[35]
N05CA	2015	thiomorpholine	TfO^-	SF	1058751 MUJXAS	100	HS	No (HS)	[35]
M02	2015	CONH-POM [a24]	-	-	-	-	-	No (HS)	[36]
O01AF	2015	OH	BF_4^-	2MeOH	1006318 OZUBAO	150	HS	Yes (211) [a25]	[37]
O01BF	2015	OH	ClO_4^-	$1.75MeOH\ 0.25H_2O$	1006319 OZUBES	150	HS / mixed	Yes (207) [a25]	[37]
O01DF	2015	OH	PF_6^-	2MeOH	1006320 OZUBIW	100	HS	No (HS) [a25]	[37]
N03AA	2016	NO_2	BF_4^-	SF	-	-	-	Yes (287)	[38]
N01AC	2016	NH_2	BF_4^-	$3MeNO_2$	1006314 EKAQUE	150	HS	No (HS) [a25]	[38]
N01BC	2016	NH_2	ClO_4^-	$3MeNO_2$	1006315 EKAJOR	150	HS	No (HS) [a25]	[38]
N02AB	2016	NMe_2	BF_4^-	$0.29H_2O$	1006316 EKAJUX	100	HS	No (HS)	[38]
N02BB	2016	NMe_2	ClO_4^-	$0.22H_2O$	1006317 EKAKAE	100	HS	No (HS)	[38]
O02DA	2016	OMe	PF_6^-	SF	1006321 EKAKEI	100	HS	No (HS)	[38]
X01AA	2016	F	BF_4^-	SF	1006322 EKAKIM	290	HS	Yes (≈240)	[38]
X01AA	2016	F	BF_4^-	SF	1006323 EKAKIM01	150	LS	Yes (≈240)	[38]
X02AA	2016	Cl	BF_4^-	SF	1006324 EKAKUY	100	LS	No (LS up to RT)	[38]

X02BA	2016	Cl	ClO_4^-	SF	-	-	-	No (LS up to RT)	[38]
C06AB	2016	COOH	BF_4^-	H_2O	-	-	-	No (LS up to RT)	[38]
S03AE	2016	S*i*Pr	BF_4^-	0.75Me_2CO	1422786 SUXHAW	250	HS	Yes (141) [a26]	[39]
S03AE	2016	S*i*Pr	BF_4^-	0.75Me_2CO	1422787 SUXHAW01	100	LS	Yes (141) [a26]	[39]
S03AC	2016	S*i*Pr	BF_4^-	0.70$MeNO_2$	1422788 XUYXUO	250	HS	Yes (174) [a26]	[39]
S03AC	2016	S*i*Pr	BF_4^-	0.70$MeNO_2$	1422789 XUYXUO01	100	LS	Yes (174) [a26]	[39]
S03AB	2016	S*i*Pr	BF_4^-	H_2O	1422790 XUYYEZ	250	HS	Yes (212) [a26]	[39]
S03AB	2016	S*i*Pr	BF_4^-	H_2O	1422791 XUYYEZ01	150	LS	Yes (212) [a26]	[39]
S03AC	2016	S*i*Pr	BF_4^-	$MeNO_2$	1422792 XUYQOB	250	HS	Yes (171) [a26]	[39]
S03AC	2016	S*i*Pr	BF_4^-	$MeNO_2$	1422793 XUYQOB01	100	LS	Yes (171) [a26]	[39]
S03AD	2016	S*i*Pr	BF_4^-	MeCN	1422794 XUYRAO	250	HS	Yes (160) [a26]	[39]
S03AD	2016	S*i*Pr	BF_4^-	MeCN	1422795 XUYRAO01	100	LS	Yes (160) [a26]	[39]
S03AD	2016	S*i*Pr	BF_4^-	MeCN	1422796 XUYRAO02	165	HS	Yes (160) [a26]	[39]
S03AD	2016	S*i*Pr	BF_4^-	MeCN	1422797 XUYRAO03	160	LS	Yes (160) [a26]	[39]
S03AA	2016	S*i*Pr	BF_4^-	SF	1422798 XUYRUI	300	HS	Yes (185) [a26]	[39]
S03AA	2016	S*i*Pr	BF_4^-	SF	1422799 XUYRUI01	100	LS	Yes (185) [a26]	[39]
S03AI	2016	S*i*Pr	BF_4^-	EtCN	1422800 SUXHEA01	100	HS	No (HS) [a26]	[39]
S03AI	2016	S*i*Pr	BF_4^-	EtCN	1422801 SUXHEA	290	HS	No (HS) [a26]	[39]
C06BE	2016	$COOH/COO^-$ [a27]	ClO_4^-	Me_2CO solv	1486674 EXAZAG	120	LS	Yes (>300)	[40]
C06BE	2016	$COOH/COO^-$ [a27]	ClO_4^-	Me_2CO solv	1486674 EXAZEK	250	LS	Yes (>300)	[40]
S03BC	2017	S*i*Pr	ClO_4^-	$MeNO_2$	1428759 GEQHUI01	250	HS	Partial (102,115)	[41]
S03BC	2017	S*i*Pr	ClO_4^-	$MeNO_2$	1428760 GEQHUI02	147	HS	Partial (102,115)	[41]
S03BC	2017	S*i*Pr	ClO_4^-	$MeNO_2$	1563026 GEQHUI	100	mixed	Partial (102,115)	[41]
S03BD	2017	S*i*Pr	ClO_4^-	MeCN	1428761 GEQGOB	250	HS	No (HS)	[41]

S03BD	2017	S*i*Pr	ClO_4^-	MeCN	1428762 GEQGOB01	140	HS	No (HS)	[41]
S03BE	2017	S*i*Pr	ClO_4^-	0.70Me_2CO	1428763 GEQGOB02	250	HS	Partial (<100)	[41]
S03BE	2017	S*i*Pr	ClO_4^-	0.70Me_2CO	1428764 GEQHES	147	HS	Partial (<100)	[41]
S03BB	2017	S*i*Pr	ClO_4^-	H_2O	1563027 GEQJAQ	250	HS	Yes (173)	[41]
S03BB	2017	S*i*Pr	ClO_4^-	H_2O	1563028 GEQJAQ01	100	LS	Yes (173)	[41]
S03BA	2017	S*i*Pr	ClO_4^-	SF	1563029 GEQJIY	250	HS	Not tested [a28]	[41]
S03BA	2017	S*i*Pr	ClO_4^-	SF	1563030 GEQJIY01	118	LS	Not tested [a28]	[41]
S03AB	2017	S*i*Pr	BF_4^-	H_2O	1564665 ZUYYEZ02	30	LS	Yes (LIESST)	[41]
S03AB	2017	S*i*Pr	BF_4^-	H_2O	1564666 ZUYYEZ03	30	HS [a2]	Yes (LIESST)	[41]
S03AD	2017	S*i*Pr	BF_4^-	MeCN	1564667 ZUYRAO04	85	LS	Yes (LIESST)	[41]
S03AD	2017	S*i*Pr	BF_4^-	MeCN	1564668 ZUYRAO06	85	HS [a2]	Yes (LIESST)	[41]
S03AD	2017	S*i*Pr	BF_4^-	MeCN	1564669 ZUYRAO05	15	HS [a2]	Yes (LIESST)	[41]
S03AC	2017	S*i*Pr	BF_4^-	$MeNO_2$	1564670 ZUYQOB03	100	LS	Yes (LIESST)	[41]
S03AC	2017	S*i*Pr	BF_4^-	$MeNO_2$	1564671 ZUYQOB02	15	LS	Yes (LIESST)	[41]
S03AC	2017	S*i*Pr	BF_4^-	$MeNO_2$	1564672 ZUYQOB04	15	HS [a2]	Yes (LIESST)	[41]
M01AH	2017	C≡C-Pt(Terpy)	BF_4^-	3.5CH_2Cl_2	1510868 JAMLOB	180	HS	No (HS)	[42]
M01AH	2017	C≡C-Pt(Terpy)	BF_4^-	10CH_2Cl_2	1510869 JAMBUX	180	LS	Yes (268)	[42]
C08BA	2017	COOMe	ClO_4^-	SF	1522449 KAQYUZ	115	HS	No (HS)	[43]
C11BD	2017	CONHtriolH_3	ClO_4^-	MeCN	1522450 KAQZAG	140	LS	Yes (>400)	[43]
C49AB	2017	chain pyrene [a29]	BF_4^-	H_2O	-	-	-	Yes (363)	[44]
C48AB	2017	chain pyrene [a30]	BF_4^-	H_2O	-	-	-	Yes (213)	[44]
N04AE	2018	NHCOMe	BF_4^-	Me_2CO	1569542 VIFXAM	240	HS	Partial (50%, 140)	[45]
N04AE	2018	NHCOMe	BF_4^-	Me_2CO	1569543 VIFXEQ	130	mixed	Partial (50%, 140)	[45]
N04BE	2018	NHCOMe	ClO_4^-	Me_2CO	1569544 VIFXIU	170	HS	No (HS)	[45]

N04BE	2018	NHCOMe	ClO_4^-	Me_2CO	1569545 VIFXIU01	120	HS	No (HS)	[45]
C06AA	2018	COOH	BF_4^-	SF	1856804 YILFAD	350	HS	Yes (345)	[46]
C06AA	2018	COOH	BF_4^-	SF	1856805 YILHAF	120	LS	Yes (345)	[46]
C06EE	2018	COOH	AsF_6^-	$2Me_2CO$	1856806 YILFEH	120	LS	Yes (>250)	[46]
C06EE	2018	COOH	AsF_6^-	Me_2CO	1856807 YILFIL	300	LS (mixed)	Yes (>250)	[46]
C06FE	2018	COOH	SbF_6^-	Me_2CO	1856808 YILFOR	300	LS (mixed)	Yes (>250)	[46]
C06FE	2018	COOH	SbF_6^-	$2Me_2CO$	1856811 YILGAE	120	LS	Yes (>250)	[46]
C06CE	2018	COOH	TfO^-	Me_2CO	1856809 YILFUX	300	LS	Yes (>350)	[46]
C06CE	2018	COOH	TfO^-	$0.5Me_2CO$	1856812 YILGEI	120	LS	Yes (>350)	[46]
C06BA	2018	COOH	ClO_4^-	SF	1856814 BIYSOT01	400	HS	Yes (380)	[46]
C10BE	2018	COOEt	ClO_4^-	$1.5Me_2CO$	1856810 YILGUY	120	LS	Yes (>300)	[46]
C10BE	2018	COOEt	ClO_4^-	$0.75Me_2CO$	1856813 YILGAE	300	LS	Yes (>300)	[46]
C03AC	2018	CH_2Br	BF_4^-	$4MeNO_2$	1854820 WIJTOB	150	LS	Yes (≈340)	[47]
C03AA	2018	CH_2Br	BF_4^-	SF	1854822 WIJVAP	200	LS	Yes (325)	[47]
C50AB	2018	chain pyrene [a31]	BF_4^-	H_2O	-	-	-	Yes (≈450)	[48]
C51AA	2018	chain pyrene [a32]	BF_4^-	SF	-	-	-	No (HS)	[48]
A10AH	2018	chain fullerene [a33]	BF_4^-	CH_2Cl_2	-	-	-	Partial (≈208)	[48]
C17AA	2018	$COOC_6H_4OMe$	BF_4^-	SF	1844100 LIPFOI	120	LS	Yes (>350)	[49]
C16AA	2018	$COOC_6H_4OH$	BF_4^-	SF	1844101 LIPFUO	120	LS	Yes (>350)	[49]
C20AB	2018	$COOC_6H_4OC_6H_{13}$	BF_4^-	H_2O	1844102 LIPGAV	120	LS	No (LS up to 350 K) [a34]	[49]
C21A	2018	$COOC_6H_4OC_{12}H_{25}$	BF_4^-	-	-	-	-	Partial (50%, 212) [a34]	[49]
C22AD	2018	$COOC_6H_4OC_{14}H_{29}$	BF_4^-	2MeCN	1844103 LIPGEZ	100	LS	Partial<10% (325) [a34]	[49]
C23AB	2018	$COOC_6H_4OC_{16}H_{33}$	BF_4^-	H_2O	1854267 LIPJIG	120	LS	Yes (>350) [a34]	[49]
C24A	2018	$COOC_6H_4OC_{18}H_{37}$	BF_4^-	-	-	-	-	Yes (>350) [a34]	[49]

C28A	2018	$COOC_{12}H_{25}$	BF_4^-	-	-	-	-	Yes (>350) [a34]	[49]
C29A	2018	$COOC_{14}H_{29}$	BF_4^-	-	-	-	-	Yes (340) [a34]	[49]
C30A	2018	$COOC_{16}H_{33}$	BF_4^-	-	-	-	-	Yes (>350) [a34]	[49]
C31A	2018	$COOC_{18}H_{37}$	BF_4^-	-	-	-	-	Yes (>350) [a34]	[49]
C14AC	2019	$CSNH_2$	BF_4^-	$2MeNO_2$	1860676 HIKPEZ01	100	LS	No (LS up to 350)	[50]
C14AC	2019	$CSNH_2$	BF_4^-	$2MeNO_2$	1860677 HIKPEZ	290	LS	No (LS up to RT)	[50]
C14BA	2019	$CSNH_2$	ClO_4^-	SF	-	-	-	No (Ls up to 350)	[50]
C15AC	2019	CSNHMe	BF_4^-	$MeNO_2$	1860678 HIKPID	100	LS	Yes (≈330)	[50]
C15AC	2019	CSNHMe	BF_4^-	$MeNO_2$	1860679 HIKPID02	290	LS	Yes (≈330)	[50]
C15AC	2019	CSNHMe	BF_4^-	$MeNO_2$	1860680 HIKPID01	330	LS (mixed)	Yes (≈330)	[50]
C15BA	2019	CSNHMe	ClO_4^-	SF	1860681 HIKRAX	102	LS	Yes (≈325)	[50]
C15BA	2019	CSNHMe	ClO_4^-	SF	1860682 HIKRAX01	290	LS	Yes (≈325)	[50]
C15BA	2019	CSNHMe	ClO_4^-	SF	1860683 HIKRAX02	370	HS	Yes (≈325)	[50]
C10BD	2019	COOEt	ClO_4^-	MeCN	1589139 WIVMEW	253	HS	Yes (233)	[51]
C37CD	2019	C≡C-anthracene [a35]	TfO^-	7MeCN	1862242 VOBCUN	100	mixed [a35]	Partial (50%, 250)	[52]
C38CC	2019	C≡C-chain [a36]	TfO^-	$18MeNO_2$ $9H_2O$	1862243 VIZSAB	180	HS	No (HS)	[52]
C19AC	2019	$COOC_6H_3(OMe)_2$	BF_4^-	$2MeNO_2$	1884423 HOSZEX	120	LS [a37]	Yes (>350)	[53]
C19AC	2019	$COOC_6H_3(OMe)_2$	BF_4^-	$2MeNO_2$	1884424 HOSZEX01	120	HS [a37]	No (HS)	[53]
C18AA	2019	$COOC_6H_3(OH)_2$	BF_4^-	SF	1884425 HOSZOH	120	LS	Unknown	[53]
C25AD	2019	$COOCH_2Ph$	BF_4^-	1.5MeCN	1884426 HOSZUN	150	LS	Yes (370)	[53]
C26AD	2019	$COOCH_2C_6H_4OMe$	BF_4^-	1.5MeCN	1884427 HOTBAW	150	LS	Not tested	[53]
C27AE	2019	$COOCH_2C_6H_3(OMe)_2$	BF_4^-	$x Me_2CO$ $0.25H_2O$	preliminary structure	120	LS	Not tested	[53]
C07BB	2019	3-COOH	ClO_4^-	$0.5H_2O$ 0.5EtOH	1910175 FOGLAR	122	LS	No (LS up to 400) [a38]	[54]
C09BA	2019	3-COOMe	ClO_4^-	SF	1910176 FOGLEV	120	LS	Not tested	[54]

C05AD	2020	CN	BF_4^-	MeCN	1961768 BADLIF	293	LS	Yes (243) [a39]	[55]
C05BA	2020	CN	ClO_4^-	SF	2010806 BADLOL	293	LS	Yes (241) [a40]	[55]
A05AA	2020	Imidazol-1-yl	BF_4^-	SF	1997944 XUYTAP	120	HS	No (HS)	[56]
A05BA	2020	Imidazol-1-yl	ClO_4^-	SF	1997945 XUYTET	120	HS	No (HS)	[56]
S03A [41]	2020	S*i*Pr	BF_4^-	[a41]	[a41]	[a41]	[a41]	[a41]	[57]
S03A [41]	2020	S*i*Pr	ClO_4^-	[a41]	[a41]	[a41]	[a41]	[a41]	[57]
S04AC	2021	S*t*Bu	BF_4^-	2.3$MeNO_2$	1991053 UKEKUT	120	LS	Yes [a42]	[58]
S04AC	2021	S*t*Bu	BF_4^-	2.3$MeNO_2$	1991052 UKEKON	250	LS / mixed	Yes [a42]	[58]
S04AC	2021	S*t*Bu	BF_4^-	0.75$MeNO_2$	1991051 UKEKIH	120	Mixed	Partial 50% (172)	[58]
S04AC	2021	S*t*Bu	BF_4^-	0.75$MeNO_2$	1991050 UKEKED	220	HS	Partial 50% (172)	[58]
S04AD	2021	S*t*Bu	BF_4^-	MeCN	1991049 UKEKAZ	120	LS	Yes (276)	[58]
S04AD	2021	S*t*Bu	BF_4^-	MeCN	1991048 UKEJUS	240	Mixed	Yes (276)	[58]
S04AD	2021	S*t*Bu	BF_4^-	MeCN	1991047 UKEJOM	250	Mixed	Yes (276)	[58]
S04AD	2021	S*t*Bu	BF_4^-	MeCN	1991046 UKEJIG	260	HS [a43]	Yes (276)	[58]
S04AE	2021	S*t*Bu	BF_4^-	1.6Me_2CO	1991045 UKEJEC	120	Mixed [a44]	Partial	[58]
S04BC	2021	S*t*Bu	ClO_4^-	$MeNO_2$	1991044 UKESUB01	120	LS	Yes (244)	[58]
S04BC	2021	S*t*Bu	ClO_4^-	$MeNO_2$	1991043 UKEHUQ	250	Mixed	Yes (244)	[58]
S04BC	2021	S*t*Bu	ClO_4^-	$MeNO_2$	1991042 UKESUB	350	HS	Yes (244)	[58]
S04BD	2021	S*t*Bu	ClO_4^-	MeCN	1991041 UKERIO05	120	LS	Yes (253)	[58]
S04BD	2021	S*t*Bu	ClO_4^-	MeCN	1991040 UKERIO04	180	LS	Yes (253)	[58]
S04BD	2021	S*t*Bu	ClO_4^-	MeCN	1991039 UKERIO03	230	LS	Yes (253)	[58]
S04BD	2021	S*t*Bu	ClO_4^-	MeCN	1991038 UKERIO02	250	Mixed	Yes (253)	[58]
S04BD	2021	S*t*Bu	ClO_4^-	MeCN	1991037 UKERIO01	290	Mixed	Yes (253)	[58]
S04BD	2021	S*t*Bu	ClO_4^-	MeCN	1991036 UKERIO	330	HS	Yes (253)	[58]

S04BE	2021	S*t*Bu	ClO_4^-	0.5Me_2CO 0.2H_2O	1991035 UKEREK	120	LS	Partial [a45]	58
S04BE	2021	S*t*Bu	ClO_4^-	0.5Me_2CO 0.2H_2O	1991034 UKERAG	250	LS	Partial [a45]	58
S04BB	2021	S*t*Bu	ClO_4^-	SF	1991033 UKEQOT01	120	LS	Not tested	58
S04BB	2021	S*t*Bu	ClO_4^-	SF	1991032 UKEQOT	250	LS	Not tested	58
C52BA	2021	$CH_2OC(O)(CH_2)_4(C_3H_5S_2)$	ClO_4^-	SF	-	-	-	Partial [a46]	59
C53BA	2021	$CONH(CH_2)_2OC(O)(CH_2)_4(C_3H_5S_2)$	ClO_4^-	SF	-	-	-	Partial [a46]	59
C54BA	2021	$COO(CH_2)_2OC(O)(CH_2)_4(C_3H_5S_2)$	ClO_4^-	SF	-	-	-	Partial [a46]	59
S07BA	2021	$S(CH_2)_2NHC(O)(CH_2)_4(C_3H_5S_2)$	ClO_4^-	SF	-	-	-	HS	59
C12BD	2021	$CONHCH_2COOH$	ClO_4^-	MeCN	2074280 ITIDOH	120	LS	Partial [a47]	59
C12BD	2021	$CONHCH_2COOH$	ClO_4^-	MeCN	2074281 ITIDOH01	330	mixed	Partial [a47]	59
C13BD	2021	$CONH(CH_2)_2COOH$	ClO_4^-	2MeCN	2074282 ITIFAV01	120	LS	Partial [a47]	59
C13BD	2021	$CONH(CH_2)_2COOH$	ClO_4^-	2MeCN	2074283 ITIFAV	290	mixed	Partial [a47]	59

[a1] personal consideration: suspected solvent loss during magnetic measurements, the $T_{½}$ is the same as the SF complex
[a2] light induced from the LS structure at the same temperature
[a3] mixed = two independent cations in the unit cell, one HS and the other LS
[a4] the complex is protonated, $[Fe(L)_2H](ClO_4)_3$·MeOH, L = bpp-4-py, the proton links together two consecutive pyridyl substituents forming a 1D chain
[a5] mixed-anion species $[Fe(L)_2](ClO_4)_x(BF_4)_{2-x}$ are also reported in the same paper
[a6] two different polymorphs that crystallize together, separated by hand at the microscope; small fraction of residual HS species
[a7] the $T_{½}$ moves to higher temperature upon increasing the number of cooling-heating cycles probably due to the loss of the MeCN solvated molecules
[a8] co-crystals with variable percentage of $[Ru(terpy)_2](BF_4)_2$ are also reported
[a9] two different polymorphs with different conformation of the CH_2SCN groups
[a10] the complex is protonated, $[Fe(L)_2H](BF_4)_3$·MeCN·H_2O, L = bpp-3-py; the spin transition at 300 K is irreversible due to loss of co-crystallized solvent; once desolvated, the $T_{½}$ moves to 240 (↑) and 231 (↓) K
[a11] propylene carbonate; the solvent-free *Z* isomer was irradiated to generate the solvent-free *E* form, which shows partial spin conversion
[a12] TTF = *E*-CH=CH-tetrathiofulvalene
[a13] cation with overall +3 charge with mono-electronic oxidation localized over the TTF moieties
[a14] $CH_2OC(O)CH_2CH_2CH_2$pyrene
[a15] the structures and the $T_{½}$ refer to three different polymorphs that interconvert each other upon heating and cooling
[a16] desolvation
[a17] the compound quickly loses the co-crystallized nitromethane molecules; only partial spin conversion is present due to the small fraction of intact solvated species, while the desolvated sample is always HS;

[a18] rapid freezing at 60 K min^{-1}
[a19] CTPZ = cyclotriphosphazene
[a20] two independent cations, one LS and one HS
[a21] the sample loses nitromethane and adsorbs two molecules of water once exposed to air, this new solvated derivative is HS at RT
[a22] disulfide bridges between two bpp ligands, the compounds are supposed to be tetranuclear species
[a23] the crystal undergoes rupture while slowly cooling to 100 K, rapid freezing blocked the complex in its HS state also at 100 K
[a24] POM = polyoxometalate $MnMo_6O_{24}$, it works also as counteranion
[a25] magnetic measurements were performed on the unsolvated samples
[a26] they all show similar $T_{½}$ around 170-180 K, similar to the SF compound, once the samples are annealed at 350 K with consequent solvent removal
[a27] The compound is formulated as $\{[Fe^{III}_3(\mu_3\text{-}O)(H_2O)_3][Fe^{II}(bppCOOH)(bppCOO)]_6\}(ClO_4)_{13}\cdot 6Me_2CO\cdot$solvate, where the deprotonated COO^- substituents of the six Fe-bpp complexes coordinate the Fe^{III}_3O cluster
[a28] single crystal obtained by annealing of the acetone solvate directly on the diffractometer
[a29] chain pyrene = $COO(CH_2)_4$pyrene
[a30] chain pyrene = $CH_2OC(O)(CH_2)_3$pyrene
[a31] chain pyrene = $COOCH_2$pyrene
[a32] chain pyrene = $CH_2OC(O)CH_2$pyrene
[a33] chain fullerene = $C_6H_4CH_2OC(O)C$(fullerene)COOEt
[a34] all samples employed for solid state magnetic measurements contain a variable degree of water, some samples may lose water during the measurements
[a35] tetranuclear species with bridging bpp ligands connected by -C≡C-anthracene-C≡C-; at 100 K, two iron centres are HS and two are LS
[a36] hexanuclear species with bridging bpp ligands connected by -C≡C-anthracene-C≡C-anthraquinone-C≡C-anthracene-C≡C-
[a37] two different polymorphs
[a38] co-crystallized solvent is lost while heating, causing an irreversible spin transition
[a39] the sample gradually loses the acetonitrile molecule forming a SF phase, which is the one SCO active
[a40] the sample employed for magnetic measurements did not belong to the same crystallographic phase of the single crystal analyzed for X-ray diffraction
[a41] continuation of the studies reported in *Chem. Eur. J.*, **2016**, *22*, 1789–1799 and *Chem. Commun.*, **2017**, *53*, 13268–13271; the solvents tested (MeCN, H_2O, $MeNO_2$ and Me_2CO) are the same; the crystal structures were collected at several temperatures upon cooling or heating; CCDC: 1976565–1975626.
[a42] irreversible spin transition at 320 K due to solvent loss.
[a43] the crystal undergoes adrupt spin transition at 255 K, while the powder sample shows a more gradual process with $T_{½}$ = 276 K
[a44] 5 independent cations in the unit cell, only one over five is HS
[a45] the magnetic measurements show the beginning of SCO above 300 K
[a46] the magnetic susceptibility starts to increase from 1-1.5 cm^3 K mol^{-1} at 150-200 K to about 3 cm^3 K mol^{-1} at 350 K
[a47] mostly LS, the magnetic susceptibility starts to increase from 0.5 cm^3 K mol^{-1} at 250 K to about 1.5 cm^3 K mol^{-1} at 350 K

Table S3 The 28 structural parameters considered for building the PCA and PLS models.

Distances	
N1–Fe	D1
N2–Fe	D2
N3–Fe	D3
N4–Fe	D4
N5–Fe	D5
N6–Fe	D6

Angles	
N1–Fe–N2	A1
N1–Fe–N3	A2
N1–Fe–N4	A3
N1–Fe–N5	A4
N1–Fe–N6	A5
N2–Fe–N3	A6
N2–Fe–N4	A7
N2–Fe–N5	A8
N2–Fe–N6	A9
N3–Fe–N4	A10
N3–Fe–N5	A11
N3–Fe–N6	A12
N4–Fe–N5	A13
N4–Fe–N6	A14
N5–Fe–N6	A15

Torsional Angles	
pyridineN1 ∠ pyrazoleN2	T1
pyridineN1 ∠ pyrazoleN3	T2
pyrazoleN2 ∠ pyrazoleN3	T3
pyridineN4 ∠ pyrazoleN5	T4
pyridineN4 ∠ pyrazoleN6	T5
pyrazoleN5 ∠ pyrazoleN6	T6
ligandN123 ∠ ligandN456	T_LL

Chemometrics methods

Principal Component Analysis (PCA)

Multivariate data analysis through PCA[60] was applied to highlight data structure and the presence of outliers, and check variability sources within the data. PCA extracts the prevailing and systematic information of the variables that describe the system by rotating the original space in a space constructed so that each new variable, called principal component (PC), is orthogonal to the others and that each new variable explains the maximum possible fraction of variance of the data not yet explained by the previous PCs. The PCs are linear combinations of the original variables, the first PC is in the direction of maximum variability of the data, the second is uncorrelated with the first (the two axes are orthogonal) and explains the maximum residual variance fraction, and so on. At maximum, as many components as the rank of the data set can be calculated, leading to exhausting the variance (information) present in the data.[61,62]

From a mathematical point of view, PCA can be written as a matrix decomposition with general formula: $\boldsymbol{X} = \boldsymbol{T}\,\boldsymbol{P}^{\boldsymbol{T}} + \boldsymbol{E}$, where $\boldsymbol{X}$ is the initial dataset, $\boldsymbol{T}$ is the matrix holding the score vectors, which are the samples coordinates in the PCs space with one score vector per each PC; $\boldsymbol{P}$ is the matrix holding the loadings vectors, which represent the weight with which each original variable contributes to the PCs. Finally, $\boldsymbol{E}$ is the matrix holding the residual variance, i.e. the part of $\boldsymbol{X}$ that is not modelled by PCA, like noise.[61]

The aspects to consider when building a PCA model are the number of PCs, the preprocessing to apply prior to PCA, how to deal with possible outliers and how to graphically interpret the results and extracting useful information, making use of Scores, Loadings and Residuals plots.

Preprocessing are a series of mathematical operations and functions that can be applied to the raw data to remove unwanted sources of variability, stabilize the model or help the interpretations.[63] Mean centring removes an offset from the data and allows focusing on the differences with respect to the average. Scaling is usually applied to make comparable variables of different nature, and scale. When the data are formed by different group of variables, each group having a different meaning and measure scale, it is useful Block-scaling to unit block variance, this scaling allows each block to contribute the same to the PCA model. It can be applied in combination with intra-block autoscaling, i.e. namely block autoscaling, which is the scaling we adopted in this work.[64]

The choice of the number of PCs is another important step to build the model. PCs are correlated to the variance explained by the model, so by taking a low number of PCs you can under-fitting your data leading in discarding some sources of variability and “lose” interesting trend/correlation. On the other hand, taking too many PCs you can over-fit your data including also unwanted information, i.e.

unsystematic sources of variability.[60] For exploratory analysis, a few components are generally sufficient, and you can still decide on the basis of the analysis of the scores how many PCs show systematic trends.[65,66]

The Scores plot is a graphical representation of the samples in space of the PCs, describing how samples are positioned according to what the components explain. Here differences, similarities, clustering or groups of samples can be observed. Since the distances between scores reflect the differences of samples in the raw data, a scores plot can be read as follows: samples corresponding to points which are located very close share similar behaviour, while points opposite with respect to the origin show opposite behaviour, and points not close, nor opposite, indicate sample which have different properties/behaviour. The Loadings plot is the representation of the weights of the original variables in the space of the PCs. As for the scores, difference and similarities among variables can be identified. In particular, variables corresponding to points which are located very close are directly correlated, while points opposite with respect to the origin indicate inverse correlation. Scores and Loadings plots for the same PCs must always be seen together and interpreted jointly. If a grouping or a trend among samples exists, the corresponding loading plot explains the reason, i.e. which are the variables mainly responsible for the observed trend, depicted by the fact that lye along the same direction in the loadings plot. Variables whose projection on the axes is very close to the origin have negligible significance.

Finally, it must be remembered that, while the direction taken by PC1 axis is unique, the sign is arbitrary, meaning the in two different PCA's of the same samples set, we can see samples in specular position in scores plot, but their relative positioning will not change (thus no inconsistency has to be considered in this case).

Partial Least Squares regression (PLS)

Partial Least Squares Regression (PLS) is one of the most known and applied methods for multivariate calibration.[67] It shares similarity with Multilinear regression (MLR) but overcomes the collinearity problem by operating a projection of the descriptors $\boldsymbol{X}$ matrix and the response $\boldsymbol{y}$ vector (PLS-1), or responses $\boldsymbol{Y}$ matrix (PLS-2) into the latent variables (LVs) space. While the other discussed projection method, PCA, operates on the $\boldsymbol{X}$ matrix determining the principal components based on the variance of $\boldsymbol{X}$ itself, PLS iteratively models both **X** and **Y** to explain as much as possible covariance of both blocks simultaneously and thus maximise the covariance between $\boldsymbol{X}$ and $\boldsymbol{Y}$. This is done by looking for a least squares solution component-wise between $\boldsymbol{t}$'s (X-scores) and $\boldsymbol{u}$'s (Y-scores), which can be schematically summarized as repeating iteratively until convergence: $\boldsymbol{T} = \boldsymbol{X}\ \boldsymbol{W}^T$; $\boldsymbol{W} = \boldsymbol{U}^T\ \boldsymbol{X}$, where the matrix $\boldsymbol{W}$ holds the PLS weights, coefficients which ensures linear

combinations of variables in $\boldsymbol{X}$ for each latent variable that maximize the covariance between $\boldsymbol{T}$ and $\boldsymbol{U}$.

Two main algorithms can be used for the calculation of the PLS models: the NIPALS algorithm and the SIMPLS algorithm, converging to the same solution.

A PLS model consists of:

- a PCA-like model for $\boldsymbol{X}$: $\boldsymbol{X} = \boldsymbol{T}\,\boldsymbol{P}^T + \boldsymbol{E}$;
- a PCA-like model for $\boldsymbol{Y}$: $\boldsymbol{Y} = \boldsymbol{U}\,\boldsymbol{Q}^T + \boldsymbol{F}$;
- the weights matrix $\boldsymbol{W}$;
- the pseudo regressions coefficients $\boldsymbol{B}$ that directly relates $\boldsymbol{X}$ with $\boldsymbol{Y}$ and can be obtained by post-processing the PLS model output: $\boldsymbol{B} = \boldsymbol{W}\,(\boldsymbol{P}^T\,\boldsymbol{W})^{-1}\,\boldsymbol{Q}^T$.

Classification (PLS-DA). Classification problems arise every time the target of a study is the establishment whether a set of samples can be classified or not in two or more classes based on a series of measured responses. The PLS-Discriminant Analysis (PLS-DA) approach uses PLS-2 regression where the $\boldsymbol{Y}$ block is formed of dummy variables encoding the class membership for each sample, i.e. for each category/class a binary $\boldsymbol{y}$ vector of 1's (sample is a member) and 0's (not a member) is the dependent variable (y).[68] The model is identical to a PLS regression model, but a criterion to assign a sample to one of the defined classes has to be decided when using PLS-DA, since the predicted values Ypred are continuous and not discrete (0 or 1) as the nominal Y. In some implementations of PLS-DA, a fixed boundary limit of 0.5 is assumed as the limit for class membership assignment. In other implementations, the threshold is optimized, as the limit giving the lowest misclassification error in cross validation. In this thesis we adopted a true discriminant rule by assigning each sample to the class for which the predicted y value is the highest. Moreover, projecting to latent variables makes obtaining a graphical representation and interpretation of the results in a similar way to PCA and PLS models possible. In the present work, PLS-DA models have been used to build prediction models of iron(II) complexes.

Validation. Multivariate Model in general requires to be tested through a process called validation, to evaluate the internal consistency and the actual predictive capabilities. These can be done with a cross-validation, in which one or a subset of samples is left out from the data set and the model is calibrated on the remaining samples. In this way, the values of the samples that are left out are predicted and so the errors are estimated. The process is repeated with another subset of samples, until every sample or subset of samples has been left out once. All the residual errors are combined in the RMSECV (Root Mean Square Error in Cross-Validation). Typical Cross Validation procedures exclude one sample at the time (LOO, Leave One Out), random or customised block of samples, whose choice depends on data and objectives. In this work we used a cross-validation scheme leaving

more samples out called venetian blind, which after defining the number of splits, ns, (a user choice parameter, the lower the more samples are left out and the more severe is the validation) keeps out at each iteration every ns samples, e.g. first iteration: left out samples are 1:ns:end sample; second iteration: 2:ns:end sample, etc…

Validation can also occur with external validation (test set), building a completely independent set of samples with respect to the ones used for calibrating the model and for which the y properties are known, and evaluating the model prediction ability on them. Generally, cross validation is used to find the optimal values of the models adjustable (or tuneable) parameters, such as the number of components in PLS and PLS-DA, while external validation allows assessing the predictive capability of a model.

Software

MATLAB Version R2019© The MathWorks, Inc., Natick, Massachusetts, USA, has been used as main platform for managing datasets, preprocessing and multivariate data analysis algorithms.

PLS_toolbox Version 8.9.1, Eigenvector Research, Inc., 3905 West Eaglerock Drive, Wenatchee, WA 98801, USA, has been used for PCA and PLS analysis of iron and cobalt complexes.

For PLS-DA analysis, a set of routines developed in MATLAB by Prof. Federico Marini (Roma, La Sapienza) and Prof. Marina Cocchi were used. Preprocessing was applied with an in-house developed routine, written in MATLAB, by Prof. Marina Cocchi.

Experimental Section

General information. Solvents – acetonitrile (MeCN) and diethyl ether (Et_2O) – and chemicals were of reagent grade and used as received. Ligand bpp-Me was synthesised as reported in the literature.[34] The elemental analyses were carried out with the Thermo Scientific Flash 2000 CHNS analyser. The infrared (IR) spectra were recorded in the Attenuated Total Reflectance (ATR) mode with the spectrophotometer Jasco FTIR-4700LE and a resolution of 2 cm^{-1}. Bands were assigned with the relative intensity: s (strong), m (medium), w (weak), vw (very weak), b (broad).

Synthesis of $[Fe(bpp\text{-}Me)_2](BF_4)_2$ (C01AA). Solid $Fe(BF_4)_2{\cdot}6H_2O$ (37.08 mg, 0.1066 mmol) was added to a colourless solution of bpp-Me (51.45 mg, 0.2284 mmol) in MeCN (3 mL) causing the immediate colour change to yellow-orange upon formation of the desired complex. After stirring for 30 minutes, the solution was filtered to eliminate undissolved materials and subjected to vapour diffusion with Et_2O (6 mL). Diffusion was complete in about one week and the X-ray quality yellow crystalline product was collected by filtration, washed with Et_2O:MeCN (2:1 *v*/*v*) and dried under vacuum. Yield: 54.07 mg (74.6%). Anal (%) calcd for $C_{24}H_{22}B_2F_8FeN_{10}$ (679.96): C 42.39, H 3.26, N 20.60. Found: C 42.71, H 3.23, N 21.03. FT-IR in ATR (KBr, cm^{-1}): 1632m + 1579m + 1523m + 1402m (*ν*C=C, *ν*C=N), 1034s (*ν*BF_4^-).

X-ray Crystal Structure Determinations. Crystal data and collection details for **C01AA** are reported in Table S3. The diffraction experiments were carried out on a Bruker APEX II diffractometer equipped with a PHOTON100 detector and using Mo-Kα radiation at 100(2) and 293(2) K. Data were corrected for Lorentz polarization and absorption effects (empirical absorption correction SADABS).[69] Structure was solved by direct methods and refined by full-matrix least-squares based on all data using F^2.[70] All non-hydrogen atoms were refined with anisotropic displacement parameters. The H atoms bonded to C-atoms were fixed at calculated positions and refined isotropically using a riding model. The program Mercury 4.3.1 was used for graphics.[71] CCDC 2191546 and 2191547 contain the supplementary crystallographic data for **C01AA** at 100 and 293 K, respectively.

These data can be obtained free of charge via https://www.ccdc.cam.ac.uk/structures/, or from the Cambridge Crystallographic Data Centre, 12 Union Road, Cambridge CB2 1EZ, UK; fax: (+44) 1223-336-033, or e-mail: deposit@ccdc.cam.ac.uk.

Table S4 Crystallographic and refinement data for **C01AA** at 100 and 293 K.

	C01AA (100 K)	**C01AA** (293 K)
Formula	$C_{24}H_{22}B_2F_8FeN_{10}$	$C_{24}H_{22}B_2F_8FeN_{10}$
M	679.98	679.98
Temperature / K	100(2)	293(2)
radiation λ / Å	Mo-Kα, 0.71073	Mo-Kα, 0.71073
Crystal system	monoclinic	monoclinic
Space group	$P2_1/n$ (n. 14)	$P2_1/n$ (n. 14)
a / Å	8.4217(4)	8.5193(9)
b / Å	8.6528(4)	8.6032(9)
c / Å	37.3757(17)	39.031(4)
β / °	93.077(2)	91.125(4)
V / Å^3	2719.7(2)	2860.2(5)
Z	4	4
D_c / g cm^{-3}	1.661	1.579
μ / mm^{-1}	0.647	0.615
F(000)	1376	1376
Colour, habit	orange, prism	orange, prism
Crystal size / mm	0.21 × 0.16 × 0.14	0.21 × 0.16 × 0.14
θ limits / °	2.183 – 26.998	2.087 – 25.049
Measured reflns	50953	49965
Independent reflns	5912	5061
Reflns with $I>2\sigma(I)$	5087	3709
R_{int}	0.0867	0.1226
R_1, wR_2 [$I>2\sigma(I)$]	0.0467, 0.0933	0.0762, 0.1933
R_1, wR_2 [all data]	0.0575, 0.0960	0.1031, 0.2062
Goodness of fit on F^2	1.165	1.073
Parameters, restraints	408, 0	408, 0
$(\Delta/\sigma)_{max}$	0.002	0.001
$\Delta\rho_{max}$, $\Delta\rho_{min}$ / e Å^{-3}	0.536, –0.547	0.754, –0.646

Table S5 Coordination bond distances (Å) and angles (°) of **C01AA** at 100 and 293 K.

parameter	100 K	293 K
Fe1–N1	1.966(2)	2.177(4)
Fe1–N3 (py)	1.895(2)	2.118(4)
Fe1–N5	1.977(2)	2.174(4)
Fe1–N6	1.974(2)	2.212(5)
Fe1–N8 (py)	1.893(2)	2.123(4)
Fe1–N10	1.961(2)	2.150(4)
N1–Fe1–N3	80.10(9)	73.60(15)
N3–Fe1–N5	79.79(9)	73.44(14)
N1–Fe1–N5 (ψ_1)	159.89(8)	146.64(14)
N6–Fe1–N8	80.05(9)	72.39(16)
N8–Fe1–N10	79.86(9)	74.00(15)
N6–Fe1–N10 (ψ_2)	159.80(8)	146.34(16)
N1–Fe1–N6	91.84(9)	94.49(17)
N1–Fe1–N8	101.11(9)	110.89(15)
N1–Fe1–N10	89.90(9)	99.12(16)
N3–Fe1–N6	100.85(9)	93.05(16)
N3–Fe1–N8 (ϕ)	178.48(10)	164.85(15)
N3–Fe1–N10	99.27(9)	120.28(15)
N5–Fe1–N6	92.21(9)	92.20(17)
N5–Fe1–N8	98.99(9)	102.29(15)
N5–Fe1–N10	93.04(9)	93.04(16)
θ [a]	89.08	89.64
Σ [b]	73.4	134.4
Θ [c]	295	467

[a] dihedral angle between the least squares planes described by the 16 C/N atoms of the bpp-Me ligands

[b] $\Sigma = \sum_{i=1}^{12} |90 - \beta_i|$, where β_i are the 12 *cis*-N−Fe−N angles about the iron atom

[c] $\Theta = \sum_{j=1}^{24} |60 - \gamma_j|$, where γ_j are the 24 unique N−Fe−N angles measured on the projection of two triangular faces of the octahedron along their common pseudo-3-fold axis

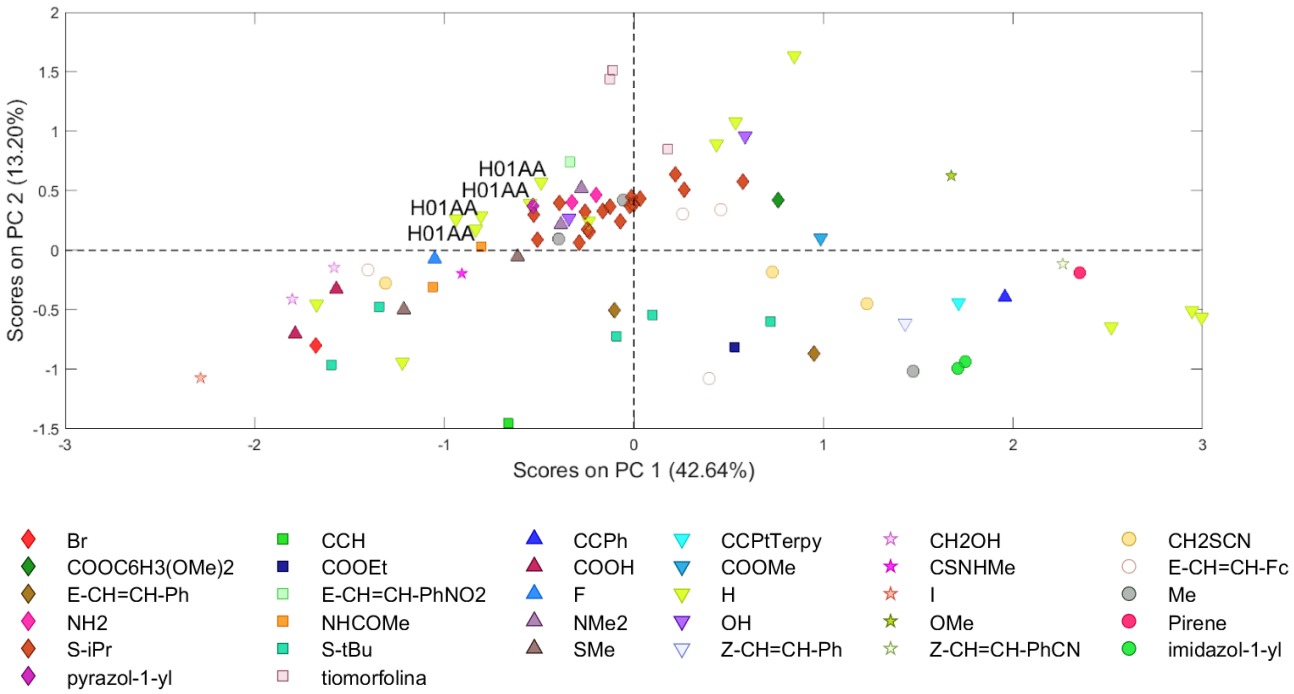

Fig. S2 PC1 *vs* PC2 Scores plot for the PCA model constructed including all the variables D, A and T for the selected 83 HS complexes; the symbol legend corresponds to the R groups, and the labels are added only for complexes directly discussed in the text.

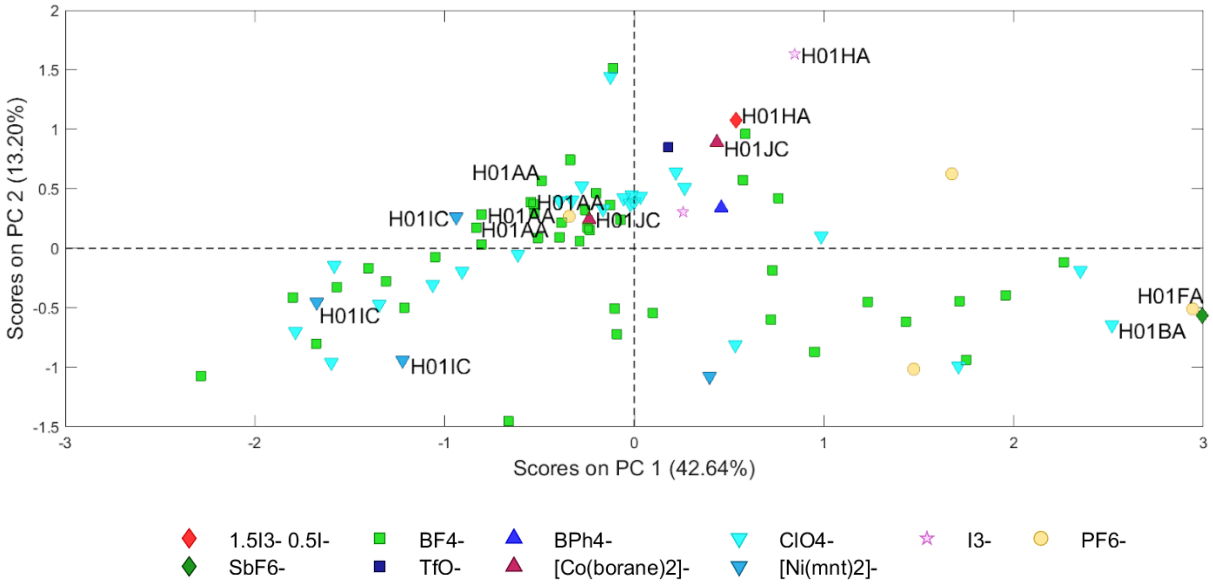

Fig. S3 PC1 *vs* PC2 Scores plot for the PCA model constructed including all the variables D, A and T for the selected 83 HS complexes; the symbol legend corresponds to the anions X^{-}, and the labels are added only for complexes directly discussed in the text.

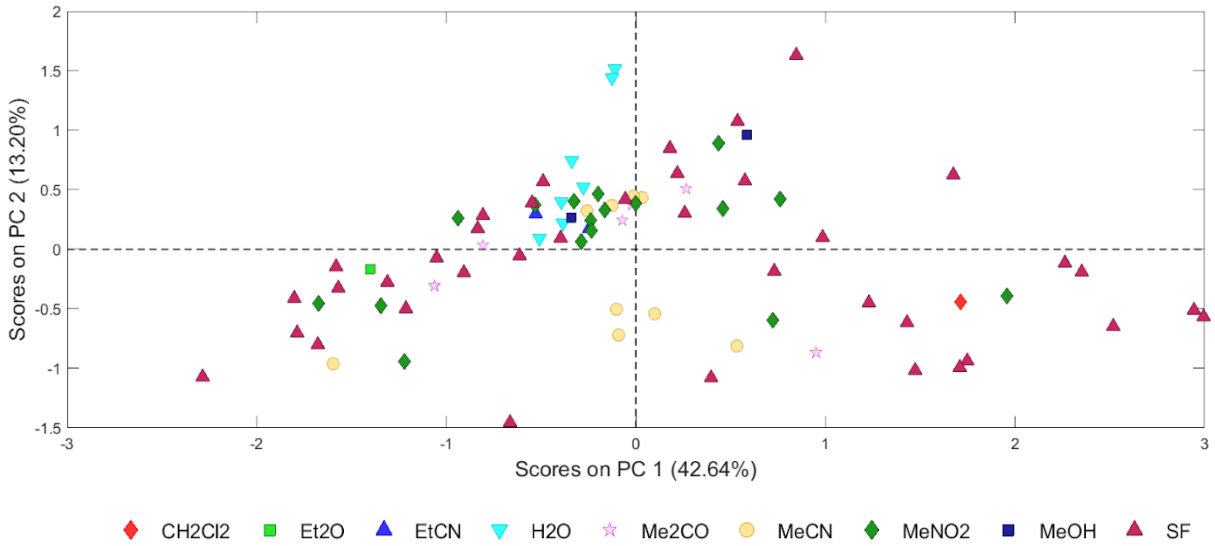

Fig. S4 PC1 *vs* PC2 Scores plot for the PCA model constructed including all the variables D, A and T for the selected 83 HS complexes; the symbol legend corresponds to the co-crystallized solvents.

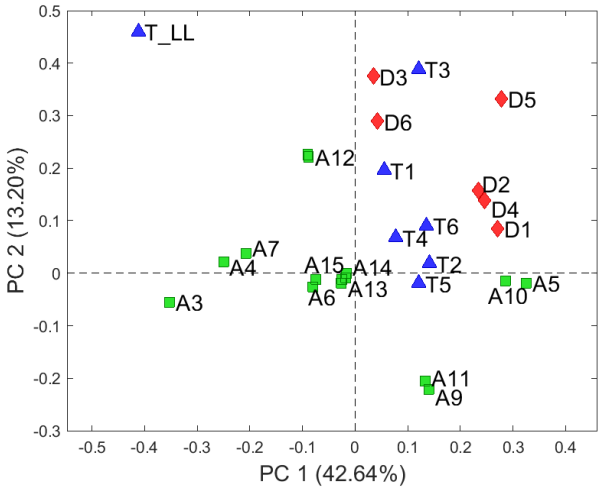

Fig. S5 PC1 vs. PC2 Loadings plot for the PCA model constructed including all the variables D, A and T for the selected 83 HS complexes; distances D are coloured in red, angles A in green and torsional angles T in blue.

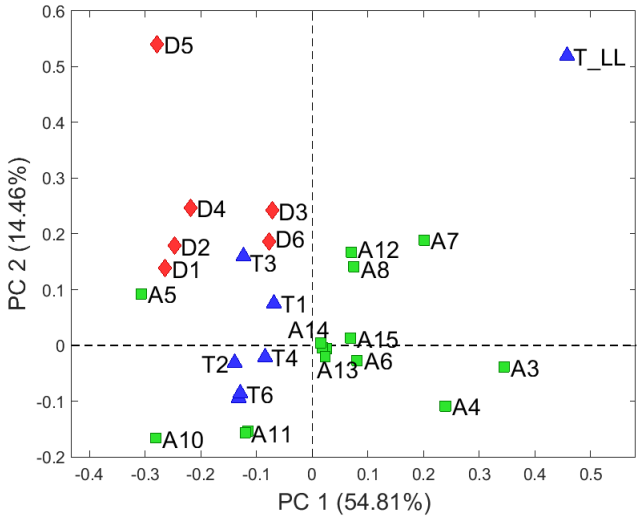

Fig. S6 PC1 vs. PC2 Loadings plot for the PCA model constructed including all the variables D, A and T for the selected 39 solvent-free (SF) HS complexes; distances D are coloured in red, angles A in green and torsional angles T in blue.

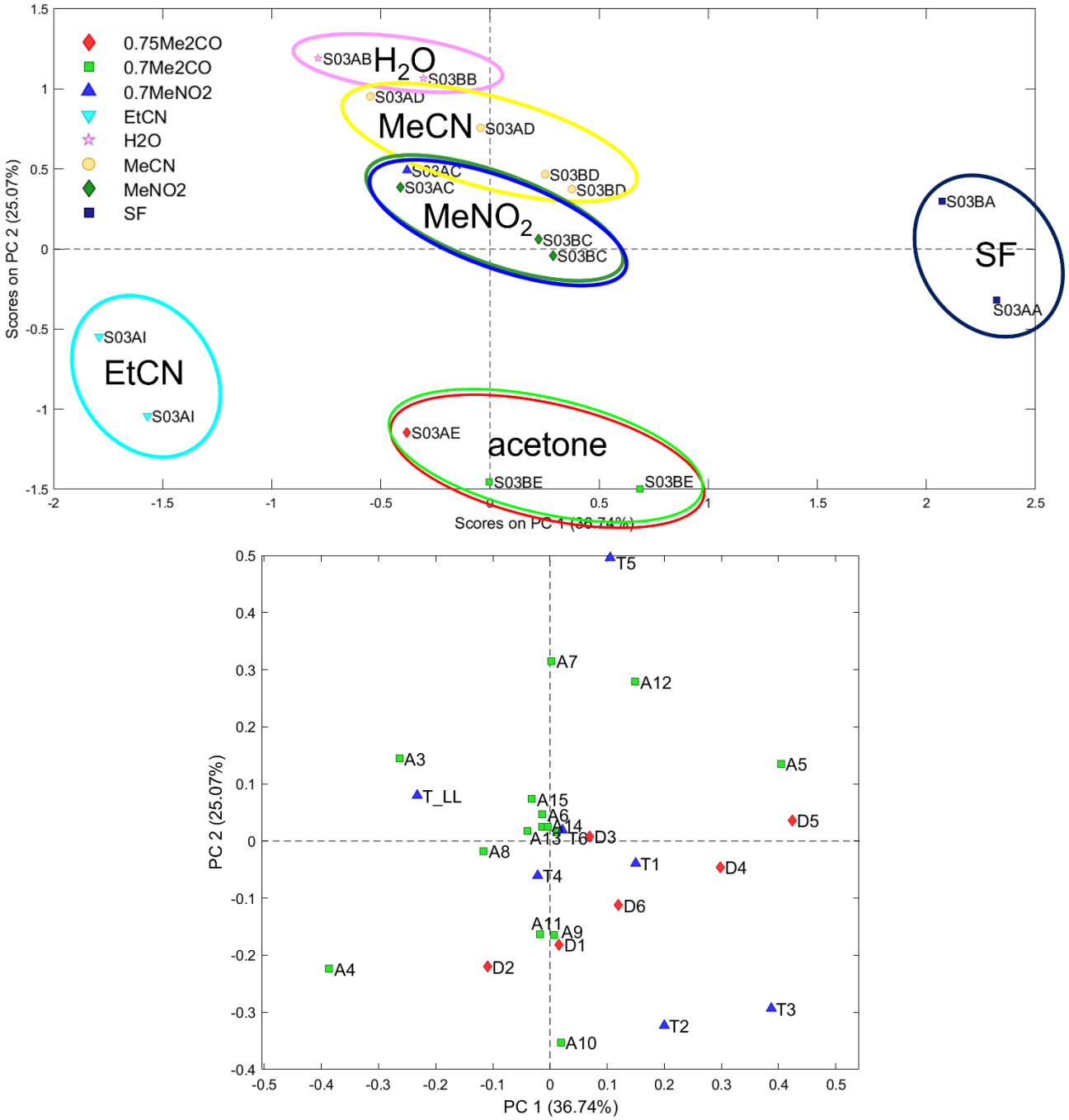

Fig. S7 PC1 *vs* PC2 Scores (top panel) and Loadings (bottom panel) plots for the PCA model constructed including all the variables D, A and T for the 17 HS complexes with R = S–*i*Pr. In the Scores plot the symbol legend corresponds to the co-crystallized solvents, and coloured circles were used to highlight complexes with the same solvent; in the Loadings plot distances D are coloured in red, angles A in green and torsional angles T in blue.

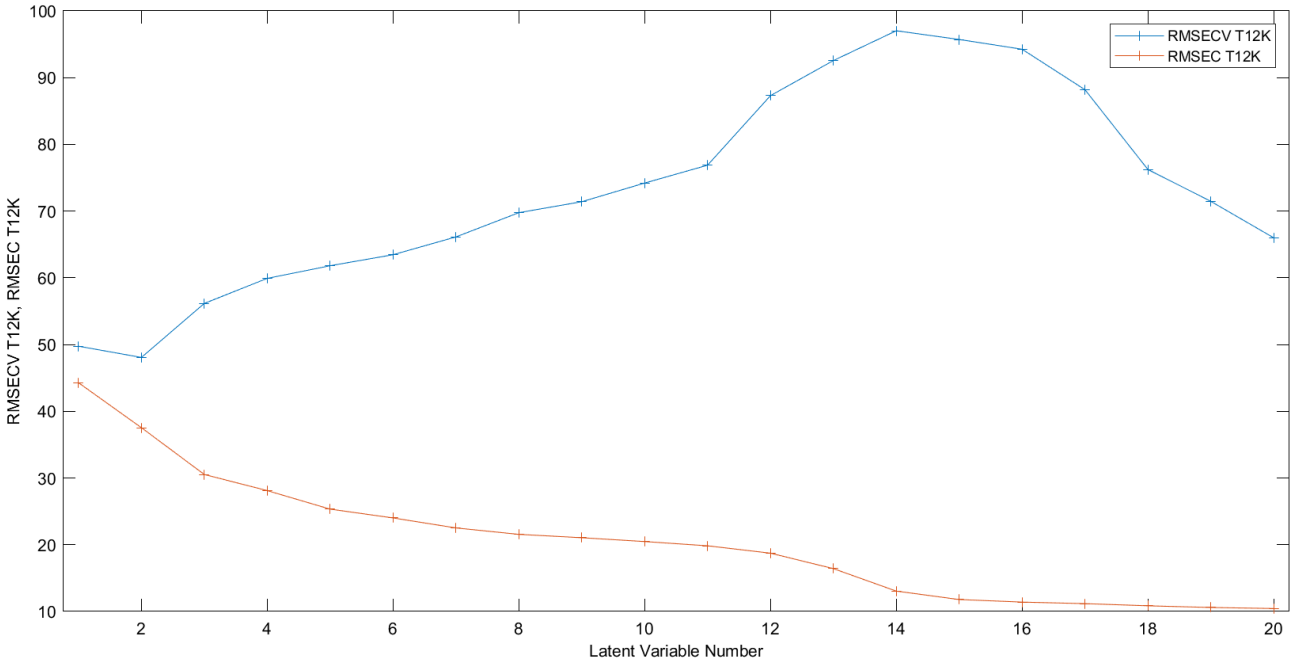

Fig. S8 Root Mean Square Errors in Calibration (RMSEC, red line) and in Cross-Validation (RMSECV, blue line) *vs* Latent Variable Number Plot.

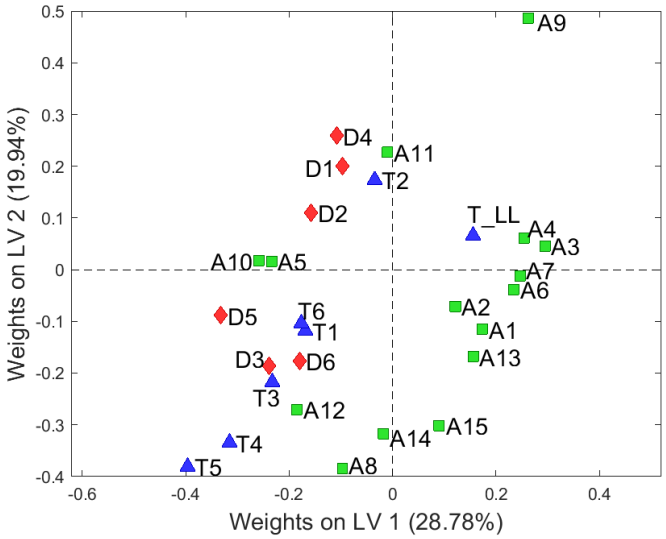

Fig. S9 PLS regression model based on 34 structures of iron(II) complexes: weights plot LV1 *vs* LV2, distances D are red diamonds, angles A are green squares, torsion angles T are blue triangles.

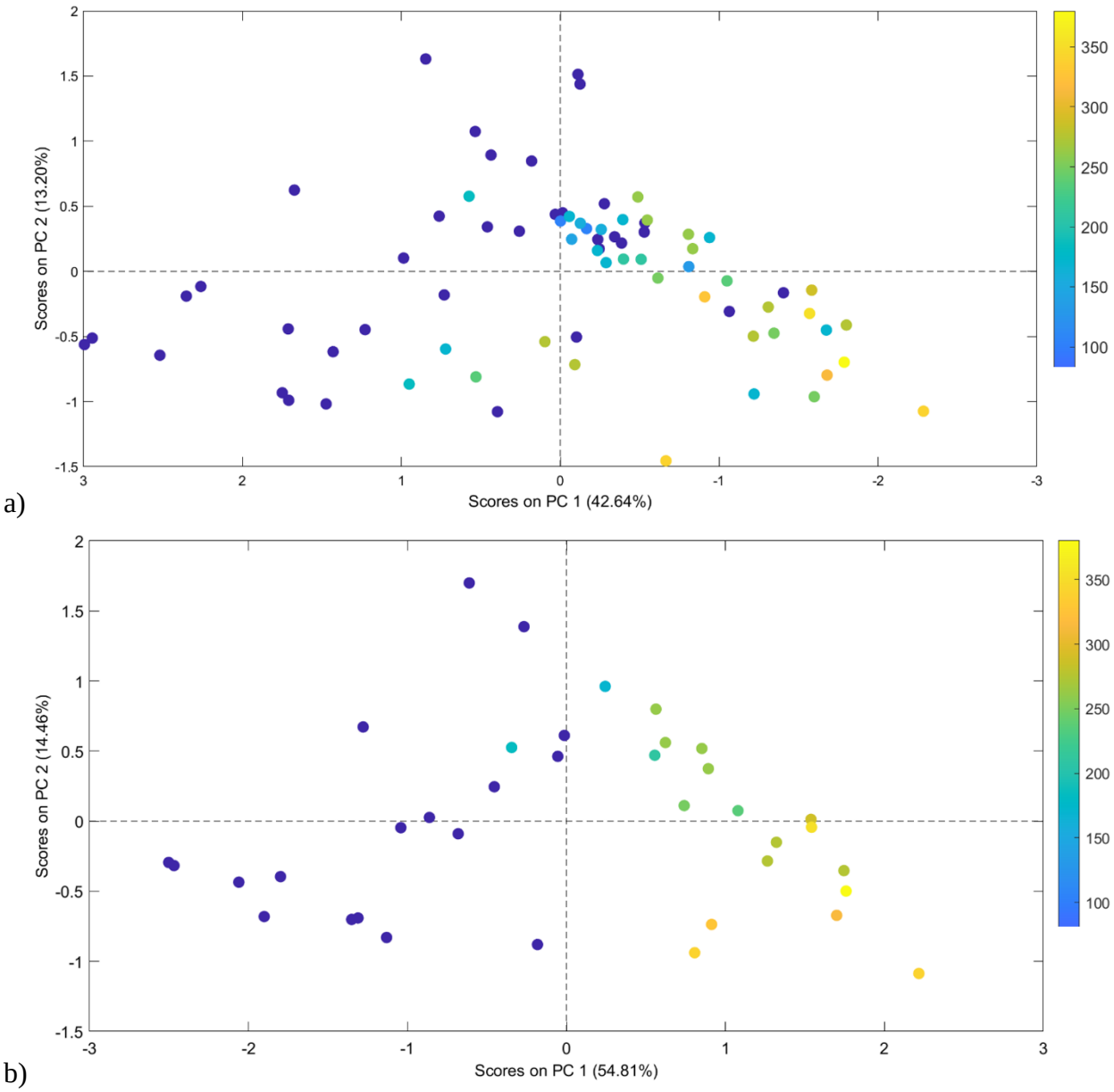

Fig. S10 $T_{½}$ values distribution in the PC1 vs PC2 Scores plots across the PCA models constructed with either a) the 83 HS complexes or b) the 39 SF HS derivatives. Dark blue circles represent the HS-blocked complexes.

References

1 J. M. Holland, C. A. Kilner, M. Thornton-Pett, M. A. Halcrow, J. A. McAllister and Z. Lu, *Chem. Commun.*, 2001, 577–578.
2 J. M. Holland, J. A. McAllister, C. A. Kilner, M. Thornton-Pett, A. J. Bridgeman and M. A. Halcrow, *J. Chem. Soc., Dalton Trans.*, 2002, 548–554.
3 V. A. Money, I. Radosavljevic Evans, M. A. Halcrow, A. E. Goeta and J. A. K. Howard, *Chem. Commun.*, 2003, 158–159.
4 V. A. Money, J. Elhaïk, M. A. Halcrow and J. A. K. Howard, *Dalton Trans.*, 2004, 1516–1518.
5 J. Elhaïk, D. J. Evans, C. A. Kilner and M. A. Halcrow, *Dalton Trans.*, 2005, 1693–1700.
6 J. Elhaïk, C. A. Kilner and M. A. Halcrow, *Dalton Trans.*, 2006, 823–830.
7 C. Carbonera, J. Sánchez Costa, V. A. Money, J. Elhaïk, J. A. K. Howard, M. A. Halcrow and J.-F. Létard, *Dalton Trans.*, 2006, 3058–3066.
8 C. Rajadurai, F. Schramm, S. Brink, O. Fuhr, M. Ghafari, R. Kruk and M. Ruben, *Inorg. Chem.*, 2006, **45**, 10019–10021.
9 C. Carbonera, Colin. A. Kilner, J.-F. Létard and M. A. Halcrow, *Dalton Trans.*, 2007, 1284–1292.
10 C. Rajadurai, Z. Qu, O. Fuhr, B. Gopalan, R. Kruk, M. Ghafari and M. Ruben, *Dalton Trans.*, 2007, 3531.
11 M. Nihei, L. Han and H. Oshio, *J. Am. Chem. Soc.*, 2007, **129**, 5312–5313.
12 M. Nihei, T. Maeshima, Y. Kose and H. Oshio, *Polyhedron*, 2007, **26**, 1993–1996.
13 N. T. Madhu, I. Salitros, F. Schramm, S. Klyatskaya, O. Fuhr and M. Ruben, *C. R. Chimie*, 2008, **11**, 1166–1174.
14 R. Chandrasekar, F. Schramm, O. Fuhr and M. Ruben, *Eur. J. Inorg. Chem.*, 2008, **2008**, 2649–2653.
15 M. Nihei, L. Han, H. Tahira and H. Oshio, *Inorg. Chim. Acta*, 2008, **361**, 3926–3930.
16 M. A. Halcrow, *Coord. Chem. Rev.*, 2009, **253**, 2493–2514.
17 C. A. Tovee, C. A. Kilner, J. A. Thomas and M. A. Halcrow, *CrystEngComm*, 2009, **11**, 2069.
18 M. Haryono, F. W. Heinemann, K. Petukhov, K. Gieb, P. Müller and A. Grohmann, *Eur. J. Inorg. Chem.*, 2009, **2009**, 2136–2143.
19 I. Šalitroš, J. Pavlik, R. Boča, O. Fuhr, C. Rajadurai and M. Ruben, *CrystEngComm*, 2010, **12**, 2361–2368.
20 M. Nihei, H. Tahira, N. Takahashi, Y. Otake, Y. Yamamura, K. Saito and H. Oshio, *J. Am. Chem. Soc.*, 2010, **132**, 3553–3560.
21 Y. Hasegawa, K. Takahashi, S. Kume and H. Nishihara, *Chem. Commun.*, 2011, **47**, 6846–6848.
22 M. Nihei, N. Takahashi, H. Nishikawa and H. Oshio, *Dalton Trans.*, 2011, **40**, 2154–2156.
23 R. González-Prieto, B. Fleury, F. Schramm, G. Zoppellaro, R. Chandrasekar, O. Fuhr, S. Lebedkin, M. Kappes and M. Ruben, *Dalton Trans.*, 2011, **40**, 7564–7570.
24 I. Šalitroš, O. Fuhr, A. Eichhöfer, R. Kruk, J. Pavlik, L. Dlháň, R. Boča and M. Ruben, *Dalton Trans.*, 2012, **41**, 5163–5171.
25 K. Takahashi, Y. Hasegawa, R. Sakamoto, M. Nishikawa, S. Kume, E. Nishibori and H. Nishihara, *Inorg. Chem.*, 2012, **51**, 5188–5198.
26 I. Šalitroš, O. Fuhr, R. Kruk, J. Pavlik, L. Pogány, B. Schäfer, M. Tatarko, R. Boča, W. Linert and M. Ruben, *Eur. J. Inorg. Chem.*, 2013, **2013**, 1049–1057.
27 Y. Hasegawa, R. Sakamoto, K. Takahashi and H. Nishihara, *Inorg. Chem.*, 2013, **52**, 1658–1665.
28 R. J. Davidson, E. W. Ainscough, A. M. Brodie, M. R. Waterland, H. R. Allcock, M. D. Hindenlang, B. Moubaraki, K. S. Murray, K. C. Gordon, R. Horvath and G. N. L. Jameson, *Inorg. Chem. Commun.*, 2013, **37**, 158–161.
29 A. Abhervé, M. Clemente-León, E. Coronado, C. J. Gómez-García and M. López-Jordà, *Dalton Trans.*, 2014, **43**, 9406–9409.
30 L. J. Kershaw Cook, H. J. Shepherd, T. P. Comyn, C. Baldé, O. Cespedes, G. Chastanet and M. A. Halcrow, *Chem. Eur. J.*, 2015, **21**, 4805–4816.
31 L. J. Kershaw Cook, R. Mohammed, G. Sherborne, T. D. Roberts, S. Alvarez and M. A. Halcrow, *Coord. Chem. Rev.*, 2015, **289–290**, 2–12.
32 L. J. Kershaw Cook, J. Fisher, L. P. Harding and M. A. Halcrow, *Dalton Trans.*, 2015, **44**, 9417–9425.
33 L. J. Kershaw Cook, R. Kulmaczewski, S. A. Barrett and M. A. Halcrow, *Inorg. Chem. Front.*, 2015, **2**, 662–670.
34 L. J. Kershaw Cook, F. L. Thorp-Greenwood, T. P. Comyn, O. Cespedes, G. Chastanet and M. A. Halcrow, *Inorg. Chem.*, 2015, **54**, 6319–6330.

35 L. Pukenas, F. Benn, E. Lovell, A. Santoro, L. J. Kershaw Cook, M. A. Halcrow and S. D. Evans, *J. Mater. Chem. C*, 2015, **3**, 7890–7896.
36 A. Abhervé, M. Palacios-Corella, J. M. Clemente-Juan, R. Marx, P. Neugebauer, J. van Slageren, M. Clemente-León and E. Coronado, *J. Mater. Chem. C*, 2015, **3**, 7936–7945.
37 L. J. Kershaw Cook and M. A. Halcrow, *Magnetochemistry*, 2015, **1**, 3–16.
38 L. J. Kershaw Cook, R. Kulmaczewski, R. Mohammed, S. Dudley, S. A. Barrett, M. A. Little, R. J. Deeth and M. A. Halcrow, *Angew. Chem. Int. Ed.*, 2016, **55**, 4327–4331.
39 L. J. Kershaw Cook, R. Kulmaczewski, O. Cespedes and M. A. Halcrow, *Chem. Eur. J.*, 2016, **22**, 1789–1799.
40 A. Abhervé, M. J. Recio-Carretero, M. López-Jordà, J. M. Clemente-Juan, J. Canet-Ferrer, A. Cantarero, M. Clemente-León and E. Coronado, *Inorg. Chem.*, 2016, **55**, 9361–9367.
41 R. Kulmaczewski, E. Trzop, L. J. Kershaw Cook, E. Collet, G. Chastanet and M. A. Halcrow, *Chem. Commun.*, 2017, **53**, 13268–13271.
42 B. Schäfer, T. Bauer, I. Faus, J. A. Wolny, F. Dahms, O. Fuhr, S. Lebedkin, H.-C. Wille, K. Schlage, K. Chevalier, F. Rupp, R. Diller, V. Schünemann, M. M. Kappes and M. Ruben, *Dalton Trans.*, 2017, **46**, 2289–2302.
43 N. Bridonneau, L. Rigamonti, G. Poneti, D. Pinkowicz, A. Forni and A. Cornia, *Dalton Trans.*, 2017, **46**, 4075–4085.
44 K. S. Kumar, I. Šalitroš, E. Moreno-Pineda and M. Ruben, *Dalton Trans.*, 2017, **46**, 9765–9768.
45 I. Capel Berdiell, R. Kulmaczewski, O. Cespedes and M. A. Halcrow, *Chem. Eur. J.*, 2018, **24**, 5055–5059.
46 V. García-López, M. Palacios-Corella, A. Abhervé, I. Pellicer-Carreño, C. Desplanches, M. Clemente-León and E. Coronado, *Dalton Trans.*, 2018, **47**, 16958–16968.
47 H. Douib, L. Cornet, J. F. Gonzalez, E. Trzop, V. Dorcet, A. Gouasmia, L. Ouahab, O. Cador and F. Pointillart, *Eur. J. Inorg. Chem.*, 2018, 4452–4457.
48 K. S. Kumar, I. Šalitroš, N. Suryadevara, E. Moreno-Pineda and M. Ruben, *Eur. J. Inorg. Chem.*, 2018, **2018**, 5091–5097.
49 I. Galadzhun, R. Kulmaczewski, O. Cespedes, M. Yamada, N. Yoshinari, T. Konno and M. A. Halcrow, *Inorg. Chem.*, 2018, **57**, 13761–13771.
50 M. Attwood, H. Akutsu, L. Martin, D. Cruickshank and S. S. Turner, *Dalton Trans.*, 2019, **48**, 90–98.
51 K. Senthil Kumar, B. Heinrich, S. Vela, E. Moreno-Pineda, C. Bailly and M. Ruben, *Dalton Trans.*, 2019, **48**, 3825–3830.
52 I. Šalitroš, R. Herchel, O. Fuhr, R. González-Prieto and M. Ruben, *Inorg. Chem.*, 2019, **58**, 4310–4319.
53 I. Galadzhun, R. Kulmaczewski and and M. A. Halcrow, *Magnetochemistry*, 2019, **5**, 9.
54 V. García-López, M. Palacios-Corella, M. Clemente-León and E. Coronado, *Polyhedron*, 2019, **170**, 95–100.
55 K. Senthil Kumar, N. Del Giudice, B. Heinrich, L. Douce and M. Ruben, *Dalton Trans.*, 2020, **49**, 14258–14267.
56 I. Capel Berdiell, R. Kulmaczewski, S. L. Warriner, O. Cespedes and M. A. Halcrow, *Eur. J. Inorg. Chem.*, 2020, **2020**, 4334–4340.
57 R. Kulmaczewski, E. Trzop, E. Collet, S. Vela and M. A. Halcrow, *J. Mater. Chem. C*, 2020, **8**, 8420–8429.
58 R. Kulmaczewski, F. Bamiduro, N. Shahid, O. Cespedes and M. A. Halcrow, *Chem. Eur. J.*, 2021, **27**, 2082–2092.
59 I. Capel Berdiell, V. García-López, M. J. Howard, M. Clemente-León and M. A. Halcrow, *Dalton Trans.*, 2021, **50**, 7417–7426.
60 I. T. Jolliffe, *Principal component analysis*, Springer, New York, 2nd ed., 2002.
61 R. Bro and A. K. Smilde, *Anal. Methods*, 2014, **6**, 2812–2831.
62 K. Varmuza and P. Filzmoser, *Introduction to Multivariate Statistical Analysis in Chemometrics*, CRC Press, Boca Raton, 1st Edition., 2016.
63 M. Li Vigni, C. Durante and M. Cocchi, in *Data Handling in Science and Technology*, Elsevier, 2013, vol. 28, pp. 55–126.
64 S. Wold, E. Johansson and M. Cocchi, *3D QSAR in drug design. Vol. 1: Theory, methods and applications / ed. by Hugo Kubinyi*, Kluwer/ESCOM, Dordrecht, the Netherlands, 1993, vol. 1.
65 R. Bro, K. Kjeldahl, A. K. Smilde and H. A. L. Kiers, *Anal. Bioanal. Chem.*, 2008, **390**, 1241–1251.
66 J. Camacho and A. Ferrer, *Chemom. Intell. Lab. Syst.*, 2014, **131**, 37–50.

67 P. Geladi and B. R. Kowalski, *Anal. Chim. Acta*, 1986, **185**, 1–17.
68 U. G. Indahl, H. Martens and T. Næs, *J. Chemometrics*, 2007, **21**, 529–536.
69 G. M. Sheldrick, *SADABS-2008/1 - Bruker AXS Area Detector Scaling and Absorption Correction, Bruker AXS, Madison, WI 2008*, .
70 G. M. Sheldrick, *Acta Crystallogr. C*, 2015, **71**, 3–8.
71 C. F. Macrae, I. Sovago, S. J. Cottrell, P. T. A. Galek, P. McCabe, E. Pidcock, M. Platings, G. P. Shields, J. S. Stevens, M. Towler and P. A. Wood, *J. Appl. Crystallogr.*, 2020, **53**, 226–235.